

Demand response program integrated with self-healing virtual microgrids for enhancing the distribution system resiliency

Motahhar Tehrani Nowbandegani^a, Mehrdad Setayesh Nazar^a, Mohammad Sadegh Javadi^b, João P.S. Catalão^{c,*}

^a Faculty of Electrical Engineering, Shahid Beheshti University, Tehran, Iran

^b Institute for Systems and Computer Engineering, Technology and Science (INESC TEC), 4200-465 Porto, Portugal

^c Research Center for Systems and Technologies (SYSTEC), Advanced Production and Intelligent Systems Associate Laboratory (ARISE), Faculty of Engineering, University of Porto, 4200-465 Porto, Portugal

ARTICLE INFO

Keywords:

Demand side management
Distributed energy resources
Energy storage systems
Resiliency
Self-healing

ABSTRACT

This paper proposes a comprehensive optimization program to increase economic efficiency and improve the resiliency of the Distribution Network (DN). A Demand Response Program (DRP) integrated with Home Energy Storage Systems (HESSs) is presented to optimize the energy consumption of household consumers. Each consumer implements a Smart Home Energy Management System (SHEMS) to optimize their energy consumption according to their desired comfort and preferences. To modify the consumption pattern of household consumers, a Real-Time Pricing (RTP) algorithm is proposed to reflect the energy price of the wholesale market to the retail market and consumers. In addition, a Self-Healing System Reconfiguration (SHSR) program integrated with Distributed Energy Resources (DER), reactive power compensation equipment, and Energy Storage Systems (ESSs) is presented to manage the DN energy and restore the network loads in disruptive events. The reconfiguration operation is performed by converting the isolated part of the DN from the upstream network to several self-sufficient networked virtual microgrids without executing any switching process. Real data of California households are considered to model the home appliances and HESSs. The proposed comprehensive program is validated on the modified IEEE 123-bus feeder in normal and emergency operating conditions.

Nomenclature

Abbreviation

AC	Air Conditioner	HESSs	Home Energy Storage Systems
DER	Distributed Energy Resources	ISO	Independent System Operator
DISCO	Distribution Company	L	Lighting system
DN	Distribution Network	MTs	Micro Turbines
DNR	Distribution Network Reconfiguration	PHEV	Plug-in Hybrid Electric Vehicle
DRP	Demand Response Program	PVs	Photo-Voltaic generators
DRPHESSs	Demand Response Program integrated with Home Energy Storage Systems	RTP	Real-Time Pricing
ELs	Essential Loads	SHEMS	Smart Home Energy Management System
ENT	Entertainment system	SHSR	Self-Healing System Reconfiguration
ESSs	Energy Storage Systems	SHSRDE	SHSR integrated with DERs, ESSs, and DN reactive power compensation equipment
EVs	Electric Vehicles	SVCs	Static VAR Compensators
		W	Washer-dryer machine
		WTs	Wind Turbines

* Corresponding author.

E-mail address: catalao@fe.up.pt (J.P.S. Catalão).

Indices and sets

$t \in T$	Index of time, $T = \{1, 2, \dots, 23, 24\}$.
$i \in J$	Index of consumers.
$d1 \in D1$	Index of smart home devices that consumers care about their power consumption at each time, $D1 = \{AC, L, ENT\}$.
$d2 \in D2$	Index of smart home devices that consumers care about the total amount of energy they use throughout the day, $D2 = \{PHEV, W\}$.
$d \in D$	Index of all smart home devices, $D = \{AC, PHEV, W, L, ENT\}$.
$Tm(i, d) \in T$	Set of times when consumer i wants to use device d .
$b, g \in B$	Index of buses.
$m, n \in Bd$	Index of buses that are disconnected from the upstream network.
$id \in Jd$	Index of consumers that are not supplied from the network.
$to \in To$	Index of time during emergency conditions.
$s \in S$	Index of scenarios.
$fs \in FS$	Index of faulted sources.
$fl \in FL$	Index of faulted lines.

Parameters

$Tempout(i, t)$	The temperature outside the house of consumer i at time t .
$\Delta(i)$	The heat transfer factor between indoor and outdoor environments of consumer i 's house.
$\nabla(i)$	The thermal efficiency of the air conditioner belongs to consumer i .
$TempComfmin(i)/TempComfmax(i)$	Minimum/Maximum comfortable temperature for consumer i .
$a(i, d)/b(i, d)$	Positive constants in the device d 's gross surplus function of consumer i .
$Pmax(i, d)$	Maximum power consumed by device d owned by consumer i .
$Emin(i, d2)/Emax(i, d2)$	Minimum/Maximum energy usage of the device $d2$ owned by consumer i .
$TempComf(i)$	The desired comfortable temperature of consumer i .
$PLightComf(i)$	The amount of power consumed to achieve the desired brightness of consumer i .
$PEntComf(i, t)$	The desired power consumption of consumer i 's entertainment system at time t .
$PHESDmax(i)$	Maximum discharge power of the HESS of consumer i .
$PHESCmax(i)$	Maximum charge power of the HESS of consumer i .
$EffPHEV(i)$	The efficiency of consumer i 's PHEV charger.
$EffHESS(i)$	The efficiency of the HESS of consumer i .
$CapHESS(i)$	The capacity of consumer i 's HESS.
$\sigma_1, \sigma_2, \sigma_3, \sigma_4$	Positive constants in the operating cost function of each HESS.
$\gamma(i)$	Minimum $SOCHES$ of consumer i that still allows the consumer to get power from the HESS.
ζ	Constant step size.
$r(b, g)/x(b, g)$	Resistance/Reactance of the line between bus b and g .
$AD(b, t, s)$	Predicted active demand at bus b at time t for scenario s .
$RD(b, t, s)$	Predicted reactive demand at bus b at time t for scenario s .
$CapMT(b), CapWT(b), CapPV(b)$	The capacity of the MT, WT, and PV at bus b .
$\omega(t), GHI(t)$	Wind speed, Global horizontal irradiance at time t .
$PRW(b, t, s)$	Predicted active output power of the WT at bus b at time t for scenario s .
$PRPV(b, t, s)$	Predicted active output power of the PV at bus b at time t for scenario s .
$CapSVC(b)$	The capacity of the SVC at bus b .
$ProbAD(b, t, s)$	Probability of scenario s for predicted active demand at bus b at time t .
$ProbRD(b, t, s)$	Probability of scenario s for predicted reactive demand at bus b at time t .
$ProbPRW(b, t, s)$	Probability of scenario s for predicted active output power of the WT at bus b at time t .
$ProbPRPV(b, t, s)$	Probability of scenario s for predicted active output power of the PV at bus b at time t .
$MTP(t)$	Price for buying active power from each MT at time t .
$MTQ(t)$	Price for buying reactive power from each MT at time t .
$CP(t)$	Price for selling energy to consumers at time t .
$UPSP(t)$	Price at wholesale spot market for selling energy to upstream network at time t .
$UPBP(t)$	Price at wholesale spot market for buying energy from the upstream network at time t .
$EFES(b)$	Charging efficiency of the ESS at bus b .
$CapES(b)$	The capacity of the ESS at bus b .
$maxSOC(b)$	Maximum state of charge of the ESS at bus b .

(continued on next column)

(continued)

$maxCES(b)/maxDES(b)$	Maximum charging/discharging power of the ESS at bus b .
$maxQWT(b)$	The coefficient for maximum output reactive power of WT at bus b .
$maxQMT(b)$	The coefficient for maximum output reactive power of MT at bus b .
$minrsv$	Minimum necessary spinning reserve of system.

Variables

$CNS(i)$	Consumer i 's net surplus.
$CGS(i)$	Consumer i 's gross surplus.
$P1(i, d1, t)$	Power consumption of device $d1$ owned by consumer i at time t .
$P2(i, d2, t)$	Power consumption of device $d2$ owned by consumer i at time t .
$PHES(i, t)$	Power consumption of HESS belongs to consumer i at time t , Positive \rightarrow Charging / Negative \rightarrow Discharging.
$Pt(i, t)$	The total power consumption of all devices owned by consumer i at time t .
$E2(i, d2)$	Energy consumption of device $d2$ owned by consumer i in simulation horizon.
$GSur(i, d1, t)$	The gross surplus consumer i gets from using device $d1$ at time t .
$GSurd(i, d2)$	The gross surplus consumer i gets from using device $d2$ throughout the day.
$Tempin(i, t)$	The temperature inside the house of consumer i at time t .
$HESSCost(i)$	The operating cost function of HESS of consumer i throughout the day.
$SOCHES(i, t)$	The state of charge for the HESS of consumer i at time t .
$Pr(t)$	Energy price in the retail market at time t .
$CostWhM(t)$	Cost of utility company for buying energy from the wholesale market at time t .
$Pl(b, g, t)$	Line transmitted active power from bus b to bus g at time t .
$Ql(b, g, t)$	Line transmitted reactive power from bus b to bus g at time t .
$Vol(b, t)$	Voltage of bus b at time t .
$PMT(b, t)$	Active generated power of the MT at bus b at time t .
$QMT(b, t)$	Reactive generated power of the MT at bus b at time t .
$PES(b, t)$	The active output power of the ESS at the bus b at time t .
$QWT(b, t)$	Reactive generated power of the WT at bus b at time t .
$QSVC(b, t)$	Reactive generated power of the SVC at bus b at time t .
$ZP(b, t)$	Binary, 1 if the WT or PV at the bus b is synchronized with the network at time t and generates active power, otherwise 0.
$ZQ(b, t)$	Binary, 1 if the WT at bus b is synchronized with the network at time t and generates or uses reactive power, otherwise 0.
$PUPB(t)$	Active power bought from the upstream network at time t .
$PUPS(t)$	Active power sold to the upstream network at time t .
$BUPB(t)$	Binary, 1 if energy is bought from the upstream network at time t , otherwise 0.
$BUPS(t)$	Binary, 1 if energy is sold to the upstream network at time t , otherwise 0.
$rsv(t)$	Spinning reserve of the system at time t .
UTP	Profit of the utility company.
$Lin(m, n)$	Binary, 0 if the energy flow in the line between buses m and n can be zero, otherwise 1.
$Din(m, to)$	Binary, 1 if the load at the bus m at time to is supplied by the network, otherwise 0.
$dsd(fl)$	Downstream demand of faulted line fl .
$nxtdsd^{nth}(fl)$	Downstream demand of n th next upstream faulted line after fl .
$ReCo_{Case}$	Resiliency coefficient for each case in emergency operation mode.
RD_{Case}	Restored demand ratio in each case in emergency operation mode.
$Resiliency$	Resiliency of the system.

1. Introduction

The cost of outages to the customer community is so high that the power system should be able to survive all usual disturbances without widespread load outages [1]. Thus, the concept of resiliency has been introduced to improve the system's efficiency in emergencies [2]. According to [3], resilience is the ability of a system to prepare and adapt to changes in conditions; and withstand and quickly recover from disruptive events. Self-healing is one of the capabilities that increase resilience and flexibility in intelligent distribution networks. Therefore, after occurring a disruptive event, an intelligent distribution network with self-healing capability can turn the distribution system into several

microgrids using reconfiguration methods [4]. Integrating DERs and a suitable method for intelligent energy management enables microgrids to restore their loads and self-sufficiently supply their demand.

Due to the high importance of the resiliency of distribution systems in recent years, the restoration of network loads after disruptive events has become a hot topic for researchers. Some papers have used the advantages of DERs to restore interrupted loads. Ref. [5] utilizes distributed energy resource management systems and renewable energy resources to adjust the frequency and voltage for the restoration of distribution systems. The two-step scenario-based model is used to utilize Renewable energy resources in the resilient operational scheduling of the system. Ref. [6] introduces an optimization process for enhancing the resiliency of the distribution system considering the interaction of DERs and loads. The method integrates the loads and DERs into a switch-level facility model to enhance the controllability of the system during outage conditions. Ref. [7] evaluates a model for increasing the dynamic stability in secondary frequency control using synchronous DERs considering the communication delay. The method encounters the time-varying communication delays in the simulation process of secondary frequency control and a delay compensator is utilized. Ref. [8] proposes a bi-level simulation process to restore islanded microgrid loads by managing frequency stability using DERs and considering network imbalance. The first level problem optimizes the restoration problem; meanwhile, the transient model is solved to manage frequency stability.

Some papers have benefited from integrating Electric Vehicles (EVs) or ESSs with DERs to improve the speed and flexibility of operation in emergencies. Ref. [9] proposes a stochastic mixed-integer linear program to improve the resiliency of the distribution system. The model uses a guidance method to send EVs to faulted areas. The restoration of Essential Loads (ELs) is done by considering the probabilistic nature of EVs availability. Ref. [10] develops a model to enhance DN resiliency in emergencies. The model uses a partitioning method for ESSs to reduce the peak load and necessary load shedding through a MILP method. Ref. [11] presents a strategy to improve the resiliency of a hydro-diesel-battery microgrid in island mode. The paper takes advantage of DERs and ESSs in the microgrid to restore high-priority loads.

Sometimes, due to the high intensity of disruptive events, a part of the system, in addition to losing its connection with the upstream network, also suffers from a shortage in its DERs and local ESSs. Also, the uncertainties related to the availability of EVs exacerbate the situation for the operators. To overcome this issue, the operators can utilize mobile energy resources and mobile storage systems in the load restoration. Mobile energy resources and mobile storage systems meliorate the load restoration process by providing energy for the isolated parts of the system suffering from resource shortage. Ref. [12] presents a preventive scheduling method to increase network resiliency and reduce the cost associated with unsupplied loads. In this method, the authors have used DERs and mobile energy resources. Meanwhile, this paper does not model the connection of the faultless part of the DN with the upstream network.

However, during highly destructive events, multiple faults, numerous unsupplied consumers, lack of sufficient resources, and weak transmission and distribution networks make it very difficult to restore service to consumers. When the generation and transmission sectors are severely limited to restoring the loads, demand-side management through appropriate DRPs is one of the effective methods for restoring system loads and increasing resilience [13]. In fact, by determining sufficient incentives for consumers, the system operator can modify their consumption pattern to utilize the capabilities of the demand side to increase resilience and operate economically effectively. Taking advantage of DSM in load restoration is one of the effective ways that has attracted the attention of researchers in recent years. Ref. [14] proposes a stochastic scenario-based model to boost DN resiliency. The model uses the DRP, solar energy resources, determination of starting points, and displacement of essential mobile energy resources to minimize the interrupted loads considering the uncertainty for solar

generation and load. Ref. [15] presents a two-stage method to decrease the disruptive impacts of pre-planned outages on a residential sector. The method integrates EV scheduling with reshaping the load curve of household consumers to minimize the unsupplied loads. Ref. [16] provides a stochastic optimization model to increase the resiliency of microgrids by modeling the uncertainties in the energy market price, renewable energy resources, and load. The model uses DERs, renewable energy resources, and interruptible and transferable loads in the scheduling of microgrids. Ref. [13] proposes a real-time pricing method in a DRP for modifying the consumption pattern of household consumers and improving the distribution system's resiliency. HESSs are utilized to supply the demand of the consumers' houses in a self-sufficient manner when the power supply from the network is interrupted.

Forming microgrids through Distribution Network Reconfiguration (DNR) is one of the most efficient and promising solutions to increase distribution system resiliency in emergencies and restore loads. Ref. [17] proposes a framework for enhancing the resiliency of the integrated power DN and district heating system. The framework uses sectionalizing switches and valves in the DNR and changes the topology of the integrated system to isolate faults and restore services. Ref. [18] develops a self-healing method to control microgrids and increase system resiliency during operation in island mode. The method uses lines and switches added to the system as backups to reduce unsupplied ELs. Ref. [19] evaluates the resiliency of DNs by introducing an index to measure the superiority of the reconfigured system. The paper focused on maximizing the restored loads and minimizing the cost associated with additional switching in the DNR. Ref. [20] proposes a restoration method for a hybrid AC-DC distribution system to increase DN resiliency. The method restores ELs in DN after a disaster by determining the output of voltage source converters and optimally planning the stored energy in electric buses in the DNR. Ref. [21] improves DN resiliency by maximizing natural gas reserves and the stored energy in EVs before the storm, applying DNR, reducing the congestion of essential lines, and directly controlling loads after the storm.

During the blackout, the black start capability of the generating unit is an essential challenge for system restoration. Ref. [22] determines the best method to restore the DN from blackouts by examining several generation units with self-starting capability. In addition, to ensure the radiality of the network topology, the optimal switching sequence during the DNR has been provided.

In emergencies, priority should be given to improving network resiliency and reducing unsupplied loads. However, the lack of attention to economic efficiency in the frameworks proposed in the literature leads to high operating costs and the inability to implement them in practice. A detailed examination of the papers mentioned above gives us the following points:

- In most of the work, only the improvement of the DN resilience has been targeted for optimization without considering the economic issues. In addition, optimizing the operation of the connected part of the network to the upstream network has not been considered.
- In most papers that have modeled the disruptive events in the system, only the outage of one line or a few limited lines has been modeled.
- The use of mobile energy resources and repair group planning increases the load restoration delay time.
- In most papers after the disaster, the black start operation has been ignored.
- The use of EVs as sources of energy after a disaster, results in the following problems: 1. The uncertainty of the availability of these cars; 2. The need to recharge immediately after exiting the emergency condition and the emergence of a new peak load; 3. The inability of the owner to use the car in emergencies and after that when charging, and as a result, damage to their comfort; 4. The need to pay incentive payments to car owners to make cars available in emergencies.

- The use of electric buses to provide energy to the network in emergencies causes the transportation network to face a shortage and exacerbates the problem during a disaster.
- In all papers that have restored the load using reconfiguration, switching has been carried out, which brings the following disadvantages: a) Time delay; b) The need for two switches on both sides of all lines in DN; c) The need to reconfigure the system again after another fault occurs; 4. Lower participation of loads in microgrids compared to the origin DN topology reduces load inertia in the system, which makes the primary frequency control more difficult.
- Almost all papers execute direct load control and load shedding as DRPs in emergencies, which severely harms the comfort of consumers.

To answer and solve the issues raised above, in this paper, a DRP integrated with HESSs (DRPHESs) to manage the energy of household consumers and a SHSR integrated with DERs, ESSs, and DN reactive power compensation equipment (SHSRDE) program to manage the energy of the DN and restore interrupted loads in emergencies is provided through the transformation of the DN into several self-sufficient networked virtual MGs. In DRPHESs, every SHEMA offers the optimal energy consumption schedule and HESSs' optimal charging and discharging schedule to each household according to the real-time prices. Furthermore, each SHEMA manages the stored energy in the HESS in emergencies to optimally supply the household appliances. In SHSRDE, ISO optimizes the active and reactive power of dispatchable resources to maximize the economic efficiency according to the network conditions. In addition, ISO dispatches the available resources and controls the equipment in the isolated part of the network to maximize the restored loads. The proposed framework has the following advantages over previous work in the field:

- In this article, a framework is presented that, in addition to improving network resiliency, simultaneously enhances the economic efficiency of operating all parts of the network (the fault-prone part that has lost its connection with the upstream network and the connected part of the network to the upstream network).
- In the model of this paper, regardless of the type of disasters, outages and faults in all types of resources, devices, and network components are considered. Also, to avoid time delays, available resources of the system are used to restore loads.
- Due to the necessity of black start management, a minimum aggregate amount of stored energy is considered in ESSs as the spinning reserve using the PJM method, so load restoration is carried out immediately and without time delay.
- Uncertainties related to renewable energy resources and load are generated through different scenarios by appropriate distribution functions. Furthermore, to speed up the optimization time, the developed backward reduction algorithm using Kantorovich distances has been used in reducing the scenario.
- Utilizing ESSs and HESSs with almost constant availability (except in cases of faults or pre-planned repairs) removes incentive payments without harming the comfort and convenience of consumers and owners of EVs. It is also shown in the paper that the initial cost of their construction will break even in less than five years.
- The restoration is done much faster without executing any switching process. In addition, if a microgrid faces another component fault, the resources available in other microgrids can supply the demand of the faulted microgrid without further reconfiguration. In addition, with the connection of microgrids, the participation of loads has increased, which causes an increase in load inertia and consequently improves the primary frequency control.
- Instead of load shedding, a pricing algorithm has been used in the DRPHESs, which according to the comfort and priority of consumers, modifies the consumption pattern of consumers to achieve

more economical operation (in normal operation conditions) and increase DN resiliency (in emergency operation conditions).

- A parameter has been introduced to measure the level of DN resiliency, which measures the system's ability to restore the loads according to the severity of the disasters in different experiences.

Table 1 makes a comparison between the works in the literature review and the proposed framework of the manuscript.

The rest of this paper is organized as follows. Section 2 explains the modeling and formulation of the proposed framework. Section 3 provides the simulation settings and results of the proposed framework. Section 4 provides a discussion of main achievements of the proposed framework. Finally, the conclusions of the paper are drawn in Section 5.

2. Modeling

2.1. Requirements description

The main security problems of power systems are caused by the imbalance between load and generation and security issues related to the transmission network.

2.1.1. Balance issues

The balance between load and generation is constantly disturbed by load fluctuations, inaccurate control of generators' output, and sometimes by the sudden outage of generation units or transmission lines. The services utilized to solve these phenomena are listed below: 1. Regulation services designed to respond to rapid load fluctuations and small unwanted changes in electricity generation; 2. Load-following services that deal with slower fluctuations; By keeping the unbalance close to zero and the frequency close to its nominal value, these two service models are considered preventive security measures. Nevertheless, the regulatory actions are relatively few, and the load-following actions are predictable. On the other hand, 3. Reserve services are for managing massive and unpredictable power shortages (which threaten system stability). Therefore, this paper will focus on the reserve services due to their importance in balance issues. Reserve services are for providing corrective actions.

2.1.2. Network issues

In a power system, the connection between generators and consumers is through an extensive network. When the load and electricity generation change, branch currents and node voltages fluctuate. The system operator can increase the amount of power transferred from one part of the network to another by using reactive power sources as voltage control services.

The amount of reactive power support service depends on the ability to supply reactive power and prevent voltage collapse after an outage occurs. Therefore, this paper will focus on reactive power support services due to their importance in network issues.

2.2. Players of the system

2.2.1. Independent system operator (ISO)

Since maintaining security and improving resiliency is a systemic concept, it should be managed centrally. Therefore, ISO is responsible for the operation of the system and the supply and purchase of the requirements for maintaining security and improving resilience.

2.2.2. Utility company

The utility company participates in the wholesale energy market on behalf of the consumers (as a retailer) and buys the energy they need. Determining the price of selling electricity to consumers is also one of the utility company's duties.

Table 1
Comparison between the Works in the Literature Review and the Proposed Framework.

References	5	6	7	8	9	10	11	12	13 (our previous article)	14	15	16	17	18	19	20	21	22	The proposed framework	
DER	✓	✓	✓	✓	✓	✗	✓	✓	✗	✓	✓	✓	✓	✓	✗	✓	✓	✓	✓	✓
ESS	✓	✗	✗	✗	✗	✓	✓	✗	✗	✗	✗	✗	✗	✗	✗	✗	✓	✗	✓	✓
DRP	✗	✓	✗	✗	✗	✓	✗	✗	✓	✓	✓	✓	✗	✗	✗	✗	✓	✗	✓	✓
HESS	✗	✗	✗	✗	✗	✗	✗	✗	✓	✗	✗	✗	✗	✗	✗	✗	✗	✗	✗	✓
DNR	✗	✓	✗	✗	✗	✗	✗	✗	✗	✓	✗	✗	✓	✓	✓	✓	✓	✓	✓	✓
RTP (reflecting the energy price in the wholesale market to the retail market)	✗	✗	✗	✗	✗	✗	✗	✗	✓	✗	✗	✗	✗	✗	✗	✗	✗	✗	✗	✓
Considering Multiple and diverse faults	✗	✗	✗	✗	✗	✗	✗	✗	✗	✗	✗	✗	✗	✗	✗	✗	✗	✗	✗	✓
Avoid direct load control (Load shedding)	✗	✗	✗	✗	✗	✗	✗	✗	✓	✗	✗	✗	✗	✗	✗	✗	✗	✗	✗	✓
Spinning reserve	✗	✗	✗	✓	✗	✓	✗	✗	✗	✗	✗	✗	✗	✗	✗	✗	✗	✓	✓	✓
Black start management	✗	✗	✗	✓	✗	✗	✗	✓	✗	✗	✗	✗	✗	✗	✗	✗	✗	✗	✓	✓
Considering uncertainties related to WTs, PVs, and demand	✓	✓	✗	✗	✓	✗	✗	✓	✗	✓	✓	✓	✓	✗	✗	✗	✗	✗	✗	✓
Avoid switching	✗	✗	✗	✗	✗	✗	✗	✗	✗	✗	✗	✗	✗	✗	✗	✗	✗	✗	✗	✓
Considering comfort and priority of consumers	✗	✗	✗	✗	✗	✗	✗	✗	✓	✗	✗	✗	✗	✗	✗	✗	✗	✗	✗	✓
Evaluating the proposed model under worst case scenarios	✗	✗	✗	✗	✗	✗	✗	✗	✓	✗	✗	✓	✗	✗	✗	✗	✗	✓	✗	✓
Simultaneous improving of network resiliency and economic efficiency	✗	✗	✗	✗	✗	✗	✓	✓	✗	✗	✗	✓	✗	✗	✗	✗	✗	✗	✗	✓
Optimizing both the connected part of DN to upstream network and the isolated part of network in emergencies	✗	✗	✗	✗	✗	✗	✗	✗	✗	✗	✗	✗	✗	✗	✗	✗	✗	✗	✗	✓

2.2.3. Distribution company (DISCO)

The ownership and operation of the distribution network resources and equipment is on DISCO. The resources and equipment in this model are Micro Turbines (MTs), Wind Turbines (WTs), Photovoltaic generators (PVs), ESSs, and Static VAR Compensators (SVCs).

2.2.4. Consumers

In this paper, all consumers are household consumers. Each consumer utilizes a SHEMS, home appliances Air Conditioner (AC), Washer-dryer machine (W), Lighting system (L), Entertainment system (ENT), a Plug-in Hybrid Electric Vehicle (PHEV), and a HESS.

2.3. DRPHESs

At the beginning of the day, SHEMSs cooperated with the utility company in implementing the DRPHESs. Each SHEMS maximizes the consumer’s net surplus by considering energy prices and settings related to consumer comfort and preferences. The utility company informs SHEMSs of the energy prices according to the total demand for each hour. This RTP program reflects wholesale market prices to consumers. Then, each SHEMS offers the optimal energy consumption schedule for each home appliance and the optimal charging and discharging schedule of the HESS. In emergencies, the energy supply to some consumers may be interrupted. In this situation, SHEMSs announces the optimal consumption schedule according to the stored energy in HESSs. Fig. 1 shows the DRPHESs flow chart.

2.4. SHSRDE

Initially, the utility company informs ISO of the network load and the energy price obtained from the DRPHESs. Moreover, DISCO informs ISO of information related to the status of system resources and equipment, such as the amount of energy stored in ESSs, failures, and pre-planned repairs. Then, by adding weather information, ISO predicts the demand and the amount of RERs generation power. Finally, ISO optimizes the active and reactive power of dispatchable resources. The objective is to maximize the utility company’s profit according to network-related constraints, network equipment and resource constraints, and system security constraints. In emergency conditions, ISO transforms the isolated part of the system into several self-sufficient networked virtual microgrids. ISO implements this process by resource dispatching and equipment control in the isolated part. The objective in

emergencies is maximizing the restored loads and number of microgrids. The SHSRDE flow chart is shown in Fig. 2.

2.5. Economic concepts

2.5.1. Consumer’s gross surplus

The consumer’s gross surplus represents the overall value that the consumer gives to the energy they buy from the utility company [23]. In this paper, each consumer considers a gross surplus for each household appliance, and the sum of all these functions for a consumer forms the gross surplus function of that consumer.

2.5.2. Consumer’s net surplus

The net surplus of each consumer is the difference between the consumer’s gross surplus and the consumer’s costs (energy purchase cost and HESS usage cost) [23]. The consumer’s net surplus expresses the additional value the consumer obtains due to the ability to purchase the entire amount of energy they need at one price.

2.5.3. Producer’s revenue

In the retail market, the utility company sells energy to household consumers. From an economic point of view, the utility company can be considered a producer in the retail market. The utility company’s (producer’s) revenue at each hour equals the hourly sold energy multiplied by the energy price per hour.

2.5.4. Global welfare

In this paper, global welfare equals the sum of the consumers’ net surplus plus the total utility company’s profit

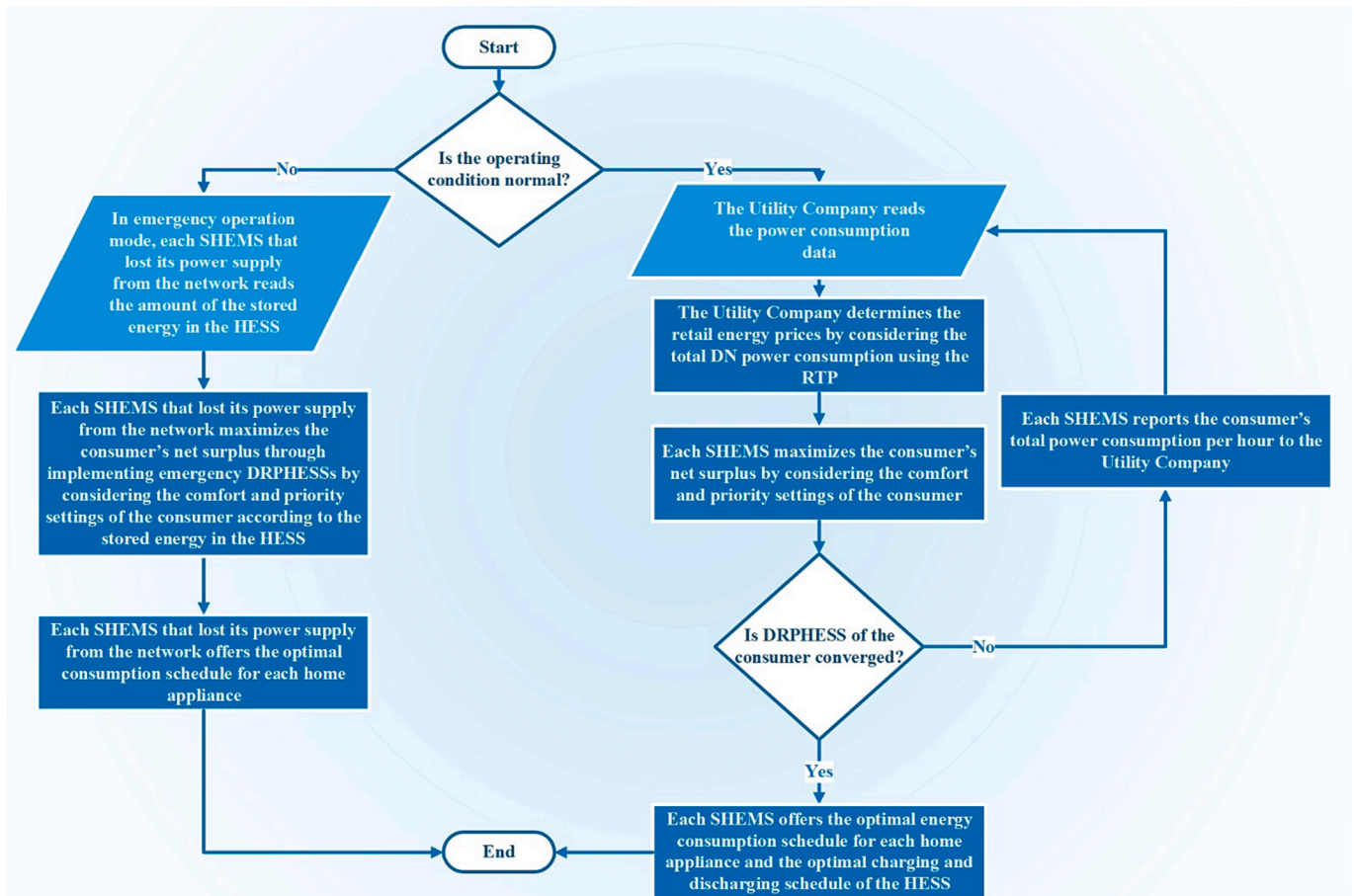


Fig. 1. The DRPHESs flow chart.

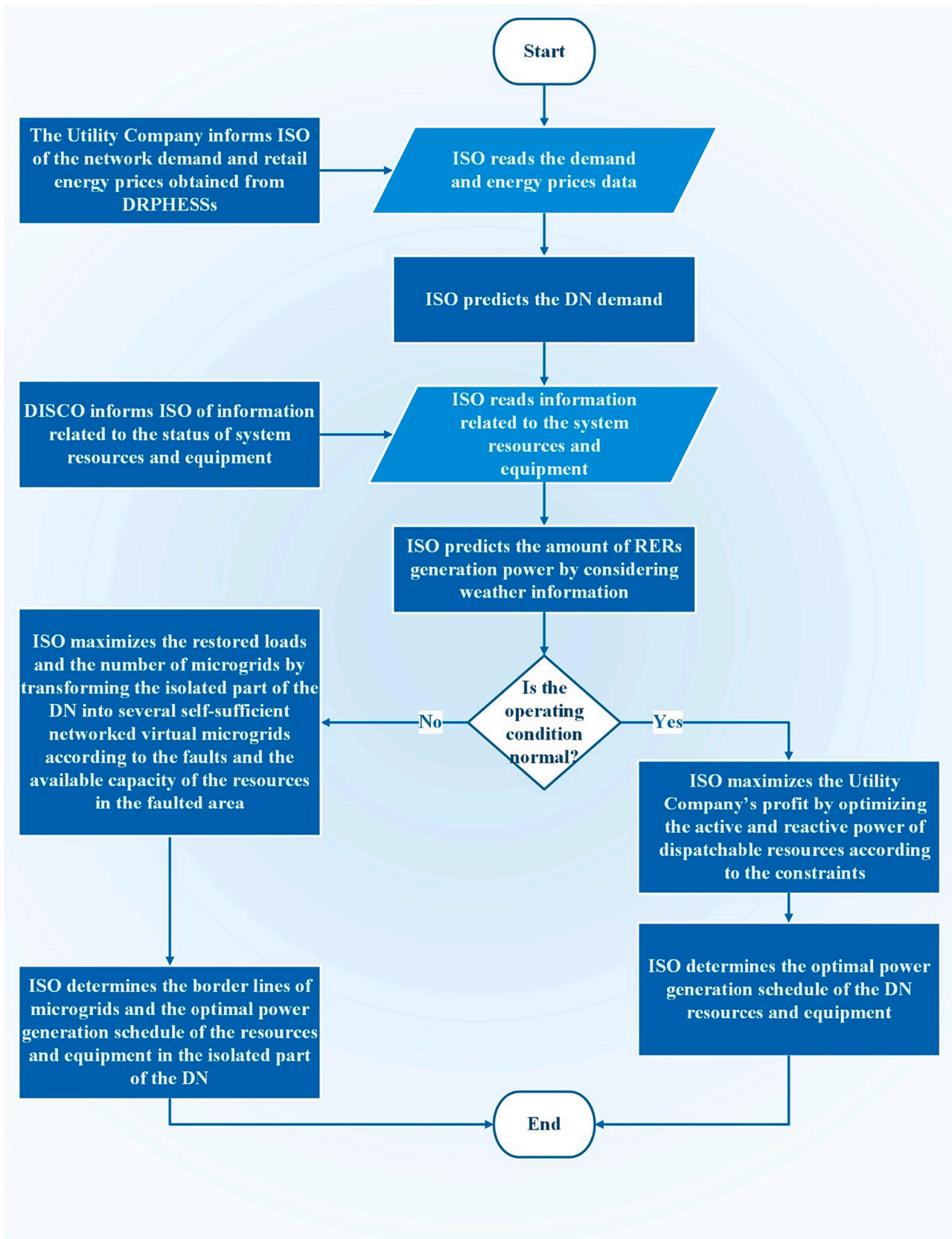


Fig. 2. The SHSRDE flow chart.

2.6. Scenario generation and reduction

Forecasting the generation of RERs is always associated with uncertainties originating from unpredictable weather conditions. The beta distribution is used in this paper to predict the amount of energy production from wind and solar energy resources [24]. In addition, the normal distribution function has been used to model the uncertainties associated with load forecasting [25].

2.6.1. Scenario generation

2.6.1.1. Wind energy resources. After the wind forecast, ISO predicts the energy produced by the wind resources according to the following linear piecewise function [24]:

$$P_{predWT}(b, t) = CapWT(b) \times \begin{cases} r_1 \omega(t) - v_{ci}; & v_{ci} \leq \omega(t) \leq v_1 \\ r_1(v_1 - v_{ci}) + r_2(\omega(t) - v_1); & v_1 \leq \omega(t) \leq v_2 \\ r_1(v_1 - v_{ci}) + r_2(v_2 - v_1) \\ + r_3(\omega(t) - v_2); & v_2 \leq \omega(t) \leq v_r \\ 1; & v_r \leq \omega(t) \leq v_{co} \\ 0; & otherwise \end{cases}, \forall t \in T, \forall b \in B \quad (1)$$

where $\omega(t)$ is the wind speed in t , $CapWT(b)$ is the capacity of the WT in bus b , $P_{predWT}(b, t)$ is the predicted generation power of the WT in bus b at time t , and $r_1, r_2, r_3, v_{ci}, v_1, v_2, v_r, v_{co}$ are positive parameters related to the technical features of WTs.

2.6.1.2. Solar energy resources. After predicting solar radiation, ISO predicts the energy produced by solar resources according to the following function [24]:

$$P_{predPV}(b, t) = CapPV(b) \times \begin{cases} \frac{GHI(t) \times 0.65}{R_c}; & 0 \leq GHI(t) < Ra_1 \\ \frac{GHI(t) \times 0.95}{R_c}; & Ra_1 \leq GHI(t) \end{cases}, \forall t \in T, \forall b \in B \quad (2)$$

where $GHI(t)$ is the global horizontal irradiance at time t , $CapPV(b)$ is the capacity of the PV in bus b , $P_{predPV}(b, t)$ is the predicted generation power of the PV in bus b at time t , and Ra_1, R_c are positive parameters related to the technical features of PVs.

The beta distribution is denoted by two positive parameters: alpha α and beta β .

$$F_{Pnorm}(x) = x^{\alpha-1} \cdot (1-x)^{\beta-1} \cdot N \quad (3)$$

$$Mean(b, t) = P_{norm}(b, t) = \frac{P_{pred}(b, t)}{Cap(b)} = \frac{\alpha}{\alpha + \beta}, \forall t \in T, \forall b \in B \quad (4)$$

$$Variance(b, t) = \sigma^2(b, t) = std^2(b, t) = \frac{\alpha\beta}{(\alpha + \beta)^2 \cdot (\alpha + \beta + 1)}, \forall t \in T, \forall b \in B \quad (5)$$

$$std(b, t) = 0.2P_{norm}(b, t) + 0.21, \forall t \in T, \forall b \in B \quad (6)$$

2.6.1.3. Demand. ISO predicts the demand according to DRPHESSs, where the mean of the normal distribution equals the demand from DRPHESSs.

2.6.2. Scenario reduction

In the simulation of this paper, 1000 scenarios are generated for each of the above variables per hour. Then, the number of scenarios for each

case per hour was reduced to 10 scenarios by the developed backward reduction algorithm using Kantorovich distances [26]. In addition to increasing the optimization speed, this algorithm also maintains the accuracy of the optimal answer.

2.7. Determination of spinning reserve

Ideally, the level of security provided by purchasing ancillary services should be determined by a cost/benefit analysis. The optimal point of this level is the equality of the marginal cost of providing more security and the marginal value of this level of security. However, calculating the marginal value of system security is an impractical task. Therefore, the PJM method, as one of the most comprehensive and practical methods, is used to evaluate the spinning reserve of the system [27]. The basis of this method is to evaluate the probability that the planned generation during the period when it is not possible to replace the generators (known as lead time) will supply the expected load. Therefore, the risk index shows the risk of providing or not providing the demand during the lead time. Finally, the spinning reserve of the system is determined based on the acceptable system's risk. The acceptable system's risk specification is a management decision based on economic and social criteria. The failure probability function is defined as follows:

$$P(failure) = 1 - e^{-\lambda \times LT} \quad (7)$$

$$LT = \frac{\text{Time to start up micro turbines}}{60\text{min} \times 24\text{hours} \times 365.5\text{days}} \quad (8)$$

where $P(failure)$ is the failure probability function, λ is the number of failures per year, and LT is the lead time.

2.8. Formulation

2.8.1. DRPHESSs

$$\max CNS(i) = \max \left(CGS(i) - HESS\text{Cost}(i) - \sum_{t \in T} Pr(t)Pt(i, t) \right) \quad (9)$$

The objective function of each consumer in DRPHESSs is maximizing their net surplus $CNS(i)$ according to (9). In (9), $CGS(i)$ is the consumer's gross surplus, $HESS\text{Cost}(i)$ is the operation cost of the HESS, and $\sum_{t \in T} Pr(t)Pt(i, t)$ is the consumer's payment to the utility company. Smart home appliances are divided into two categories: 1. The smart home appliances that consumers care about their power consumption at each time, $D1 = \{AC, L, ENT\}$, 2. The smart home appliances that consumers care about the total amount of energy they use throughout the day, $D2 = \{PHEV, W\}$. Hence, the gross surplus functions of the first category appliances are dependent on their power consumptions at each time. However, the gross surplus functions of the second category depend on the total amount of energy they use throughout the day.

Furthermore, in the proposed schedule of each SHEMS for the first category of household appliances, the optimal consumption power is suggested to the consumer. While, for the second category of household appliances, optimal energy consumption is suggested to the consumer. This means that the consumer will know when to use his washing-drying machine, or when to charge his electric vehicle battery.

The indoor temperature of each consumer in each hour is defined in equation (10):

$$\begin{aligned} Tempin(i, t) &= Tempin(i, t-1) + \Delta(i)(Tempout(i, t) \\ &\quad - Tempin(i, t-1)) + \nabla(i)P1(i, AC, t), \forall i \\ &\in J, \forall t \in T \end{aligned} \quad (10)$$

where $Tempin(i, t)$ is the indoor temperature of consumer i 's house at t , $Tempout(i, t)$ is the outdoor temperature of consumer i 's house at time t , and $\Delta(i)$ is the heat transfer factor between the indoor and outdoor

environments of the consumer i 's house. $\nabla(i)$ shows the thermal efficiency of the air conditioner belongs to the consumer i , and $P1(i, AC', t)$ is the power consumption of the AC belongs to consumer i at time t .

The limitation on the minimum and maximum comfort temperature of the consumer's house is shown in equation (11):

$$TempComfmin(i) \leq Tempin(i, t) \leq TempComfmax(i), \forall i \in J, \forall t \in Tm(i, AC') \quad (11)$$

where $TempComfmin(i)$ and $TempComfmax(i)$ are the minimum and maximum comfortable temperature for consumer i , respectively.

Equations (12) and (13) are the power consumption constraints of ACs:

$$0 \leq P1(i, AC', t) \leq Pmax(i, AC'), \forall i \in J, \forall t \in Tm(i, AC') \quad (12)$$

$$P1(i, AC', t) = 0, \forall i \in J, \forall t \in T \setminus Tm(i, AC') \quad (13)$$

where $Pmax(i, AC')$ is the maximum power consumption limit on the AC of consumer i .

Equations (14) and (15) are the gross surplus function of each consumer's AC:

$$GSur(i, AC', t) = a(i, AC') - b(i, AC')(Tempin(i, t) - TempComf(i))^2, \forall i \in J, \forall t \in Tm(i, AC') \quad (14)$$

$$GSur(i, AC', t) = 0, \forall i \in J, \forall t \in T \setminus Tm(i, AC') \quad (15)$$

where $TempComf(i)$ is the desired comfortable temperature of consumer i . In addition, $a(i, AC')$ and $b(i, AC')$ are positive constants. This function is defined as a differentiable and concave function of $Tempin(i, t)$ in a way that when the temperature inside the house is equal to the desired temperature of the consumer, the gross surplus of the consumer is maximized. When the difference between the desired comfort temperature and the inside temperature increases, the gross surplus of the consumer decreases.

Equations (16) and (17) are the limitations of the PHEV power consumption of each consumer:

$$0 \leq P2(i, PHEV', t) \leq Pmax(i, PHEV'), \forall i \in J, \forall t \in Tm(i, PHEV') \quad (16)$$

$$P2(i, PHEV', t) = 0, \forall i \in J, \forall t \in T \setminus Tm(i, PHEV') \quad (17)$$

where $P2(i, PHEV', t)$ is the power consumption of consumer i 's PHEV at time t , and $Pmax(i, PHEV')$ is the maximum power limit on consumer i 's PHEV.

Equation (18) shows the minimum and maximum PHEV energy consumption during the simulation day:

$$EminPHEV(i) \leq \sum_{t \in Tm(i, PHEV')} EffPHEV(i) P2(i, PHEV', t) \leq EmaxPHEV(i), \forall i \in J \quad (18)$$

where $EminPHEV(i)$ and $EmaxPHEV(i)$ are the limits on minimum and maximum energy usage of consumer i 's PHEV, and $EffPHEV(i)$ is the efficiency of consumer i 's PHEV charger.

Equation (19) is the PHEV gross surplus function of each consumer:

$$GSurtd(i, PHEV') = a(i, PHEV') E2(i, PHEV') + b(i, PHEV'), \forall i \in J \quad (19)$$

where $E2(i, PHEV')$ is the energy consumption of consumer i 's PHEV. In addition, $a(i, PHEV')$ and $b(i, PHEV')$ are positive constants. The consumers only care about their PHEVs to be charged to a certain level within a specified time ($Tm(i, PHEV')$). This function is defined as a differentiable and concave function of $E2(i, PHEV')$ in a way that the gross surplus of the consumer's PHEV is maximized when the electric

vehicle battery is fully charged. The higher the energy stored in the PHEV's battery, the higher the gross surplus of the consumer.

Equations (20) and (21) show Ws' power consumption limits:

$$0 \leq P2(i, W', t) \leq Pmax(i, W'), \forall i \in J, \forall t \in Tm(i, W') \quad (20)$$

$$P2(i, W', t) = 0, \forall i \in J, \forall t \in T \setminus Tm(i, W') \quad (21)$$

where $P2(i, W', t)$ is the power consumption of consumer i 's W at time t , and $Pmax(i, W')$ is the maximum power limit on consumer i 's W. Equation (20) is defined for this purpose so that the power consumption in the optimization of SHEMS does not exceed its maximum limit. This does not mean that the power consumption of the washing machine can be changed during its operation. Because the minimum time for optimization in this article is 1 h, this may be misunderstood. If this equation is not defined for the SHEMS, it may determine the suggested hourly energy consumption more than the permissible limit, which is contradictory to the reality. These issues are also true for equation (16).

Equation (22) shows the minimum and maximum energy consumption for the Ws during the simulation day:

$$EminW(i) \leq \sum_{t \in Tm(i, W)} P2(i, W', t) \leq EmaxW(i), \forall i \in J \quad (22)$$

where $EminW(i)$ and $EmaxW(i)$ are the limits on minimum and maximum energy usage of consumer i 's W.

Equation (23) defines the W gross surplus function of each consumer:

$$GSurtd(i, W') = a(i, W') E2(i, W') + b(i, W'), \forall i \in J \quad (23)$$

where $E2(i, W')$ is the energy consumption of consumer i 's W. In addition, $a(i, W')$ and $b(i, W')$ are positive constants. This function is defined as a differentiable and concave function of $E2(i, W')$. Each consumer cares about cleaning the desired amount of clothes using their washing machine. The more clothes cleaned in the washing-drying machine, the higher the consumer's gross surplus from using W. Hence, according to the assumptions and based on the proposed formulation, the gross surplus of the consumer improves as the energy consumption of the W increases, and more of the consumer's clothes become cleaner.

Equations (24) and (25) are the limitations of the power consumption of the Ls:

$$0 \leq P1(i, L', t) \leq Pmax(i, L'), \forall i \in J, \forall t \in Tm(i, L') \quad (24)$$

$$P1(i, L', t) = 0, \forall i \in J, \forall t \in T \setminus Tm(i, L') \quad (25)$$

where $P1(i, L', t)$ is the power consumption of consumer i 's L at time t , and $Pmax(i, L')$ is the maximum power consumption of consumer i 's L.

Equations (26) and (27) define the gross surplus function of each consumer's L:

$$GSur(i, L', t) = a(i, L') - b(i, L')(P1(i, L', t) - PLightComf(i, t))^2, \forall i \in J, \forall t \in Tm(i, L') \quad (26)$$

$$GSur(i, L', t) = 0, \forall i \in J, \forall t \in T \setminus Tm(i, L') \quad (27)$$

where $PLightComf(i, t)$ the amount of power consumed to achieve the desired brightness of consumer i at time t . In addition, $a(i, L')$ and $b(i, L')$ are positive constants. This function is defined as a differentiable and concave function of $P1(i, L', t)$ in a way that when the consumer house's brightness is equal to their desired brightness, the gross surplus of the consumer's L is maximized. When the difference between the desired and obtained brightness increases, the gross surplus of the consumer decreases.

Equations (28) and (29) show the power consumption limits of the consumers' ENTs:

$$0 \leq P1(i, Ent', t) \leq Pmax(i, Ent'), \forall i \in J, \forall t \in Tm(i, Ent') \quad (28)$$

$$P1(i, Ent', t) = 0, \forall i \in J, \forall t \in T \setminus Tm(i, Ent') \quad (29)$$

where $P1(i, Ent', t)$ is the power consumption of consumer i 's Ent at time t , and $Pmax(i, Ent')$ is the limit on maximum power consumption of consumer i 's Ent.

Equations (30) and (31) define the gross surplus function of each consumer's ENT:

$$GSur(i, Ent', t) = a(i, Ent') - b(i, Ent')(P1(i, Ent', t) - PEntComf(i, t))^2, \forall i \in J, \forall t \in Tm(i, Ent') \quad (30)$$

$$GSur(i, Ent', t) = 0, \forall i \in J, \forall t \in T \setminus Tm(i, Ent') \quad (31)$$

where $PEntComf(i, t)$ is the desired power consumption of the consumer i 's entertainment system at time t . In addition, $a(i, L')$ and $b(i, L')$ are positive constants. This function is defined as a differentiable and concave function of $P1(i, Ent', t)$ in a way that when the consumer ENT's power consumption is equal to their desired power consumption, the gross surplus of the consumer's L is maximized. When the difference between the desired and real power consumption increases, the gross surplus of the consumer decreases.

Equation (32) is the cost of operating each consumer's HESS:

$$HEssCost(i) = \sigma_1 \sum_{i \in T} (PHEss(i, t))^2 - \sigma_2 \sum_{i=1}^{23} (PHEss(i, t)PHEss(i, t+1)) + \sigma_3 \sum_{i \in T} (\min(SOCHEss(i, t) - \gamma(i)CapHEss(i), 0))^2 + \sigma_4, \forall i \in J \quad (32)$$

of the shelf life of the HESS.

Equation (33) is the limitation on the maximum charging and discharging power of HESSs:

$$PHEssDmax(i) \leq PHEss(i, t) \leq PHEssCmax(i), \forall i \in J, \forall t \in T \quad (33)$$

where $PHEssDmax(i)$ is the limit on maximum discharging power and $PHEssCmax(i)$ is the limit on maximum charging power of consumer i 's HESS.

Equation (34) represents the SOC of HESSs per hour:

$$SOCHEss(i, t) = SOCHEss(i, t-1) - \left(\frac{EffHEss(i)PHEss(i, t)}{CapHEss(i)} \right), \forall i \in J, \forall t \in T \quad (34)$$

where $EffHEss(i)$ is the efficiency of the HESS of consumer i , and $CapHEss(i)$ is the capacity of consumer i 's HESS.

Equation (35) is the acceptable range of HESSs' SOC:

$$0 \leq SOCHEss(i, t) \leq 1, \forall i \in J, \forall t \in T \quad (35)$$

Equation (36) represents the minimum stored energy in HESSs for the next day:

$$SOCHEss(i, t) \geq 0.4, \forall i \in J, \forall t \in T | t \geq 24 \quad (36)$$

Equation (37) defines the total power consumption of each consumer per hour:

$$Pt(i, t) = \sum_{d1 \in D1} P1(i, d1, t) + \sum_{d2 \in D2} P2(i, d2, t), \forall i \in J, \forall t \in T \quad (37)$$

Equation (38) defines the cost function of the utility company:

$$CostWhM(t) = \begin{cases} cc_{11} \left(\sum_{i \in J} Pt(i, t) \right)^2 + cc_{12} \left(\sum_{i \in J} Pt(i, t) \right) + cc_{13}; 0 \leq \sum_{i \in J} Pt(i, t) \leq X_1 \\ cc_{21} \left(\sum_{i \in J} Pt(i, t) \right)^2 + cc_{22} \left(\sum_{i \in J} Pt(i, t) \right) + cc_{23}; X_1 \leq \sum_{i \in J} Pt(i, t) \leq X_2 \\ \vdots \\ cc_{k1} \left(\sum_{i \in J} Pt(i, t) \right)^2 + cc_{k2} \left(\sum_{i \in J} Pt(i, t) \right) + cc_{k3}; X_{k-1} \leq \sum_{i \in J} Pt(i, t) \leq X_k \end{cases}, \forall t \in T \quad (38)$$

where $PHEss(i, t)$ is the power consumption of HESS belongs to consumer i at time t , if this variable is positive the HESS is charging and if this variable is negative the HESS is discharging. $SOCHEss(i, t)$ is the state of charge of consume i 's HESS at time t . $CapHEss(i)$ is the capacity of consumer i 's HESS, and $\gamma(i)$ shows the minimum $SOCHESS$ of consumer i that still allows the consumer to get power from the HESS. In addition, $\sigma_1, \sigma_2, \sigma_3, \sigma_4$ are positive constants in the operating cost function of each HESS. The first term of (32) presents the destructive effect of fast charging and discharging on the HESS. The second term denotes that if the values of $PHEss(i, t)$ and $PHEss(i, t+1)$ have different signs, an additional cost will be imposed. The third term presents that the available energy level of HESS should be greater than a predefined minimum value, which is denoted by $\gamma(i)$. Finally, the fourth term shows the effect

Equation (39) is the real-time energy price determined by the utility company:

$$Pr^n(t) = \frac{\partial CostWhM(t)}{\partial \sum_{i \in J} Pr^{n-1}(i, t)}, \forall t \in T \quad (39)$$

For each hour, the utility company sets the price of selling energy to consumers equal to the marginal cost of buying it from the wholesale market.

Equations (40), (41), and (42) optimize the power consumption of smart home appliances and the charging and discharging power of HESSs in each iteration of the algorithm according to the real-time prices:

$$P1^n(i, d1, t) = P1^{n-1}(i, d1, t) + \zeta \left(\frac{\partial GSur^{n-1}(i, d1, t)}{\partial P1^{n-1}(i, d1, t)} - Pr^n(t) \right), \forall i \in J, \forall d1 \in D1, \forall t \in Tm(i, d1) \quad (40)$$

$$P2^n(i, d2, t) = P2^{n-1}(i, d2, t) + \zeta \left(\frac{\partial GSurt^{n-1}(i, d2, t)}{\partial P2^{n-1}(i, d2, t)} - Pr^n(t) \right), \forall i \in J, \forall d2 \in D2, \forall t \in Tm(i, d2) \quad (41)$$

$$PHEss^n(i, t) = PHEss^{n-1}(i, t) - \zeta \left(\frac{\partial HEssCost^{n-1}(i)}{\partial PHEss^{n-1}(i, t)} + Pr^n(t) \right), \forall i \in J, \forall t \in T \quad (42)$$

Equation (43) represents the gross surplus of each consumer.:

$$CGS(i) = \sum_{d1 \in D1} \sum_{t \in T} GSur(i, d1, t) + \sum_{d2 \in D2} GSurt(i, d2, t), \forall i \in J \quad (43)$$

In normal operating conditions, the objective function of each consumer is (9) and constraints are (10)-(43).

Equations (44) and (45) indicate that for each consumer who lost the power supply from the network during emergencies, the HESS supplies the demand for their home appliances:

$$PHEssDmax(id) \leq PHEss(id, to) \leq 0, \forall id \in Jd, \forall to \in To \quad (44)$$

$$PHEss(id, to) + Pt(id, to) = 0, \forall id \in Jd, \forall to \in To \quad (45)$$

The objective function and constraints of the DRPHESs in emergency conditions are the same as in normal operating conditions, in addition to (44) and (45). However, only the consumers whose power supply has been interrupted from the upstream network cooperate in emergency DRPHESs. Therefore, the objective function and constraints are implemented on $\forall to \in To$ instead of $\forall t \in T$.

2.8.2. SHSRDE

$$\max UTP = \max \left[\begin{array}{l} \left(\sum_{t \in T} \left(\sum_{b \in B} \left(\sum_{s \in S} CP(t) ProbAD(b, t, s) \times AD(b, t, s) \right) + BUPS(t) UPSP(t) PUPS(t) \right) \right) \\ - \left(\sum_{t \in T} \left(\left(\sum_{b \in B} (MTP(t) PMT(b, t) + MTQ(t) QMT(b, t)) \right) + BUPB(t) UPBP(t) PUPB(t) \right) \right) \end{array} \right] \quad (46)$$

The objective function of SHSRDE in normal operating conditions (46) is to maximize the profit of the utility company. $CP(t)$ is the price for selling energy to consumers at time t , $ProbAD(b, t, s)$ is the probability of scenario s for predicted active demand at bus b at time t , and $AD(b, t, s)$ is the predicted active demand at bus b at time t for scenario s . $BUPS(t)$ is a binary variable that equals 1 if energy is sold to the upstream network at time t , otherwise it equals to 0. $UPSP(t)$ is the price at wholesale spot market for selling energy to the upstream network at time t , and $PUPS(t)$ is the active power sold to the upstream network at time t . $MTP(t)$ and $MTQ(t)$ are the prices for buying active and reactive power from each MT at time t , respectively. $PMT(b, t)$ and $QMT(b, t)$ are the active and reactive generated power of the MT at bus b at time t , respectively. $BUPB(t)$ is a binary variable that equals 1 if energy is bought from the upstream network at time t , otherwise it equals to 0. $UPBP(t)$ is the price

at wholesale spot market for buying energy from upstream network at time t , and $PUPB(t)$ is the active power bought from the upstream network at time t . The first part of (46) shows the utility company's revenue from the sale of electricity to household customers and the upstream network. The second part of (46) represents the utility company's cost of purchasing power from MTs and the energy market.

Equation (47) is the limitation of purchased power from the upstream network (the variable is in kW):

$$0 \leq PUPS(t) \leq 1000, \forall t \in T \quad (47)$$

Equation (48) indicates the maximum charging and discharging power of ESSs.

$$- \max CES(b) \leq PES(b, t) \leq \max DES(b), \forall t \in T, \forall b \in B \quad (48)$$

where $PES(b, t)$ is the active output power of the ESS at the bus b at time t . $\max CES(b)$ and $\max DES(b)$ are maximum charging and discharging power of the ESS at bus b , respectively.

The state of charge of ESSs per hour is defined in equation (49):

$$SOC(b, t) = SOC(b, t-1) - \left(\frac{EFES(b) PES(b, t)}{CapES(b)} \right), \forall t \in T, \forall b \in B \quad (49)$$

where $EFES(b)$ is the charging efficiency of the ESS at bus b , and $CapES(b)$ is the capacity of the ESS at bus b .

Equations (50) and (51) represent the constraints related to the stored energy in ESSs and the minimum stored energy in ESSs for the next day:

$$0 \leq SOC(b, t) \leq \max SOC(b), \forall t \in T, \forall b \in B \quad (50)$$

$$SOC(b, t) \geq 0.5 \times \max SOC(b), \forall t \in T | t \geq 24, \forall b \in B \quad (51)$$

where $\max SOC(b)$ is the maximum state of charge of the ESS at bus b .

Equation (52) indicates the voltage of each bus for each hour:

$$Vol(b, t) - Vol(g, t) = r(b, g) Pl(b, g, t) + x(b, g) Ql(b, g, t), \forall t \in T, \forall b, g \in B \quad (52)$$

where $Vol(b, t)$ is the voltage of bus b at time t . $r(b, g)$ and $x(b, g)$ are the

resistance and reactance of the line between bus b and g . $Pl(b, g, t)$ and $Ql(b, g, t)$ are the line transmitted active and reactive power from bus b to bus g at time t , respectively.

Equation (53) represents the minimum and maximum stability voltage of each bus:

$$0.95 \leq Vol(b, t) \leq 1.05 \quad (53)$$

Equations (54) and (55) indicate the active and reactive power balance in the lines:

$$Pl(b, g, t) + Pl(g, b, t) = 0, \forall t \in T, \forall b, g \in B \quad (54)$$

$$Ql(b, g, t) + Ql(g, b, t) = 0, \forall t \in T, \forall b, g \in B \quad (55)$$

Equations (56) and (57) indicate the active power flow in the lines:

$$\sum_{s \in S} (ProbPRW(b, t, s)PRW(b, t, s) + ProbPRPV(b, t, s)PRPV(b, t, s)) + PES(b, t) + PMT(b, t) - \sum_{s \in S} ProbAD(b, t, s)AD(b, t, s) = \sum_{g \in B} Pl(b, g, t), \forall t \in T, \forall b \in B | b \leq 122, |r(b, g) > 0 \tag{56}$$

$$BUPB(t)PUPB(t) - BUPS(t)PUPS(t) = \sum_{g \in B} Pl(b, g, t), \forall t \in T, \forall b \in B | b \geq 123, |r(b, g) > 0 \tag{57}$$

where $ProbPRW(b, t, s)$ is the probability of scenario s for predicted active output power of the WT at bus b at time t , and $PRW(b, t, s)$ is the predicted active output power of the WT at bus b at time t for scenario s . $ProbPRPV(b, t, s)$ is the probability of scenario s for predicted active

According to (61), for each t , the power is either bought from the upstream network or sold to it, and simultaneous implementation of both is not feasible:

$$BUPB(t)BUPS(t) = 0, \forall t \in T \tag{61}$$

Equation (62) shows the limitation of the reactive power produced by wind energy resources due to their power factor:

$$-\max_{s \in S} QWT(b) \sum_{s \in S} ProbPRW(b, t, s)PRW(b, t, s) \leq QWT(b, t) \leq \max_{s \in S} QWT(b) \sum_{s \in S} ProbPRW(b, t, s)PRW(b, t, s), \forall t \in T, \forall b \in B \tag{62}$$

output power of the PV at bus b at time t , and $PRPV(b, t, s)$ is the predicted active output power of the PV at bus b at time t for scenario s .

In the simulation, the bus specified with the number 123 is the bus connected to the upstream network feeder.

Equation (58) represents the reactive power flow in the lines:

where $\max_{s \in S} QWT(b)$ the coefficient for maximum output reactive power of WT at bus b .

Equations (63) and (64) respectively indicate the system's spinning reserve for each time and the minimum required spinning reserve of the

$$QWT(b, t) + QSVC(b, t) + QMT(b, t) - \sum_{s \in S} ProbRD(b, t, s)RD(b, t, s) = \sum_{g \in B} Ql(b, g, t), \forall t \in T, \forall b \in B | b \leq 122, |r(b, g) > 0 \tag{58}$$

where $QWT(b, t)$ is the reactive generated power of the WT at bus b at time t . $QSVC(b, t)$ is the reactive generated power of the SVC at bus b at time t . $ProbRD(b, t, s)$ is the probability of scenario s for predicted reactive demand at bus b at time t , and $RD(b, t, s)$ is the predicted reactive demand at bus b at time t for scenario s .

Equations (59) and (60) respectively indicate the constraints of active and reactive power balance in the network for each hour:

system for each hour:

$$rsv(t) = \sum_{b \in B} SOC(b, t)CapES(b), \forall t \in T \tag{63}$$

$$rsv(t) \geq \min rsv, \forall t \in T \tag{64}$$

Equations (65) and (66) indicate the limitations of the maximum and minimum active and reactive (according to the power factor) power produced by MTs:

$$\sum_{b \in B} \left(\sum_{s \in S} (ProbPRW(b, t, s)PRW(b, t, s) + ProbPRPV(b, t, s)PRPV(b, t, s)) + PES(b, t) + PMT(b, t) \right) + BUPB(t)PUPB(t) = \sum_{b \in B} \left(\sum_{s \in S} ProbAD(b, t, s)AD(b, t, s) \right) + BUPS(t)PUPS(t), \forall t \in T \tag{59}$$

$$\sum_{b \in B} (QWT(b, t) + QSVC(b, t) + QMT(b, t)) \tag{60}$$

$$0 \leq PMT(b, t) \leq CapMT(b), \forall t \in T, \forall b \in B \tag{65}$$

$$-\max_{s \in S} QMT(b)PMT(b, t) \leq QMT(b, t) \leq \max_{s \in S} QMT(b)PMT(b, t), \forall t \in T, \forall b \in B \tag{66}$$

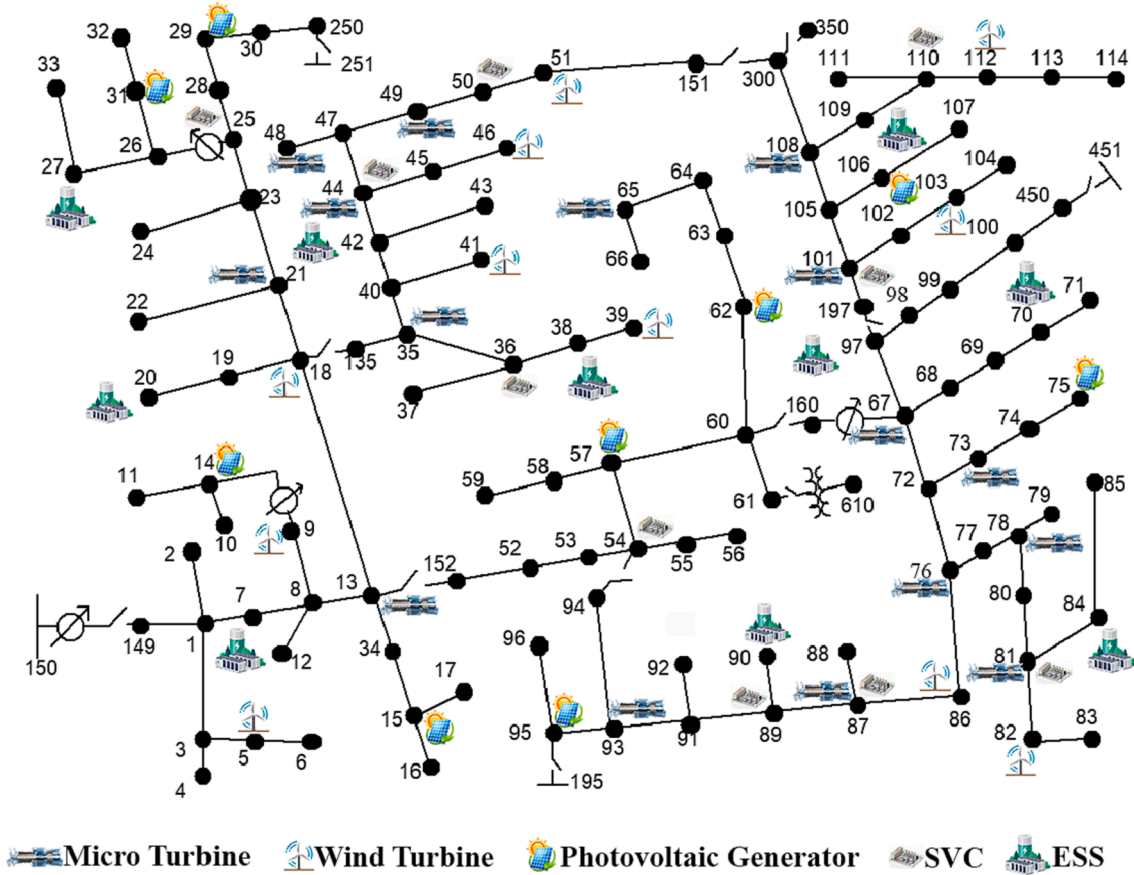


Fig. 3. Modified IEEE 123-bus feeder.

Table 2
Location and Capacity of Resources and Equipment.

Type	[Location (Bus No), Capacity (kW), and for SVCs (kVAr)]
MT	[13,80], [21,180], [35,120], [44,140], [48,100], [49,160], [65,120], [67,110], [73,140], [76,140], [78,120], [81,80], [87,140], [93,120], [101,150], [108,40]
WT	[5,80], [9,60], [18,100], [39,80], [41,30], [46,80], [51,95], [82,60], [86,100], [103,85], [112,50]
PV	[14,60], [15,60], [29,60], [31,80], [57,40], [62,80], [75,60], [95,40], [106,40]
SVC	[25,100], [36,100], [44,100], [50,100], [54,100], [81,100], [87,100], [89,100], [101,100], [110,100]
ESS	[7,100], [20,150], [27,90], [38,200], [42,300], [70,150], [84,150], [90,60], [97,200], [109,200]

where $Cap_{MT}(b)$ is the capacity of the MT at bus t , and $max_{QMT}(b)$ is the coefficient for maximum output reactive power of MT at bus b .

Equation (67) is related to the output reactive power of SVCs:

$$-Cap_{SVC}(b) \leq Q_{SVC}(b, t) \leq Cap_{SVC}(b), \forall t \in T, \forall b \in B \quad (67)$$

where $Cap_{SVC}(b)$ is the capacity of the SVC at bus b .

In normal operating conditions, the objective function of SHSRDE (46) aims to maximize the profit of the utility company subjected to (47)-(67).

Equation (68) is the objective function of SHSRDE in emergency operating conditions:

$$\max \left[\sum_{m \in B} \sum_{t \in T} \sum_{s \in S} Din(m, to) (AD(m, to, s) + RD(m, to, s)) + \sum_{m \in B} \sum_{n \in B | r(m, n) > 0} (1 - Lin(m, n)) \right] \quad (68)$$

where $Din(m, to)$ is a binary variable that equals 1 if the load at the bus m at time to is supplied by the network, otherwise it equals to 0. $Lin(m, n)$ is a binary variable that equals to 0 if the energy flow in the line between buses m and n can be zero, otherwise it equals to 1. The first part of (68) aims to maximize the restored load; meanwhile, the second part tries to maximize the number of self-sufficient microgrids in the isolated section of the network.

Equations (69) and (70) determine whether each network line can be a microgrid border, in other words, whether it is possible to zero the transmitted power through these lines:

$$Pl(m, n, to) = Lin(m, n)Pl(m, n, to), \forall m, n \in B | r(m, n) > 0, \forall to \in T \quad (69)$$

$$Ql(m, n, to) = Lin(m, n)Ql(m, n, to), \forall m, n \in B | r(m, n) > 0, \forall to \in T \quad (70)$$

Equation (71) represents the resiliency coefficient for each case:

$$ReCo_{Case} = \left[\frac{\sum_{fs \in FS} FaultedSourceCapacity(fs)}{\sum_{m \in Bd} SourceCapacity(m)} + \frac{\sum_{fl \in FL} n_{xt} d_{sd}^{n-1th}(fl) \cdot n_{xt} d_{sd}^{1st}(fl) \cdot d_{sd}(fl)}{\sum_{fl \in FL} n_{xt} d_{sd}^{nth}(fl) \cdot \dots \cdot n_{xt} d_{sd}^{2nd}(fl) \cdot n_{xt} d_{sd}^{1st}(fl)} \right] \quad (71)$$

The first part of (71) shows the ratio of faulted resources to all available resources in the system. The second part of (71) shows the severity of the

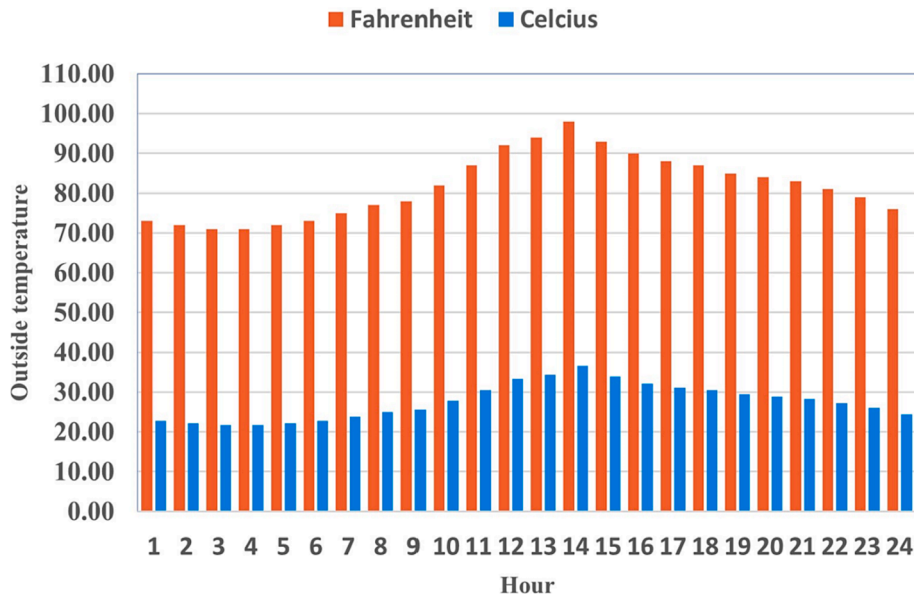


Fig. 4. The hourly temperature in the simulation area [29].

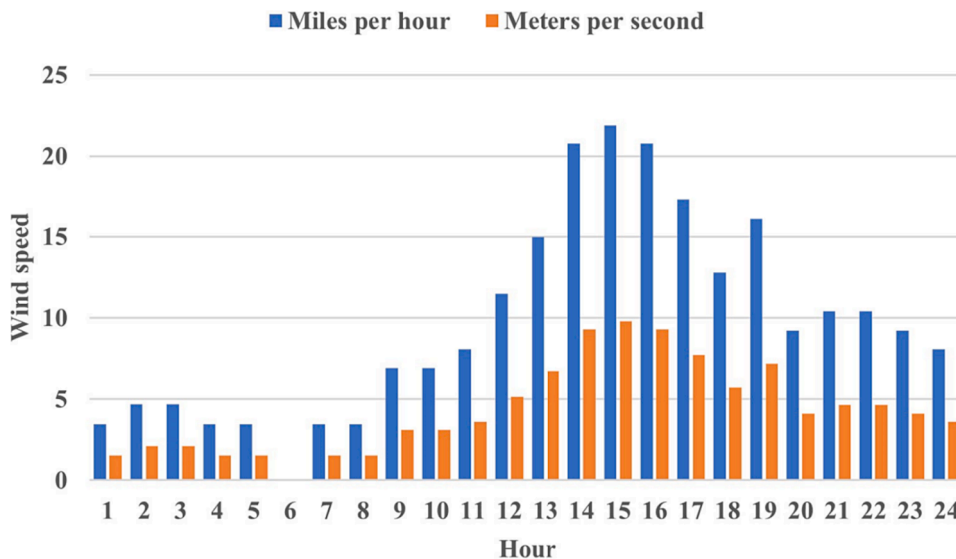


Fig. 5. The hourly wind speed in the simulation area [30].

line faults in terms of the downstream load of the line fault and hierarchical faults in the communication path between the consumer and the upstream network.

The ratio of restored load in each case is defined in equation (72):

$$RL_{Case} = \frac{\sum_{m \in B} \sum_{t \in T} \sum_{s \in S} Din(m, to) (ProbAD(b, t, s)AD(m, to, s) + ProbRD(b, t, s)RD(m, to, s))}{\sum_{m \in B} \sum_{t \in T} \sum_{s \in S} (AD(m, to, s) + RD(m, to, s))} \tag{72}$$

Equation (73) shows the network resiliency in emergency conditions according to: 1. the number and severity of faults and outages and 2. the ratio of the restored load in the isolated section:

$$Resiliency = \frac{\sum_{Cases} (ReCo_{Case} \times RL_{Case})}{\sum_{Cases} ReCo_{Case}} \tag{73}$$

In emergency operating conditions, the objective function of SHSRDE is (68) subjected to (48)-(56), (58)-(60), (62)-(67), and (69)-(73). However, these constraints are implemented on $\forall to \in To$ (i.e., during emer-

gency conditions) instead of $\forall t \in T$ (i.e., during a day) and $\forall m, n \in Bd$ (i.e., the set of buses isolated from the upstream network) instead of $\forall b, g \in B$ (i.e., all of the buses). In addition, in the constraints of this step, instead of $AD(b, t, s)$ and $RD(b, t, s)$, the expressions $Din(m)AD(m, to, s)$ and $Din(m)RD(m, to, s)$ are replaced, respectively.

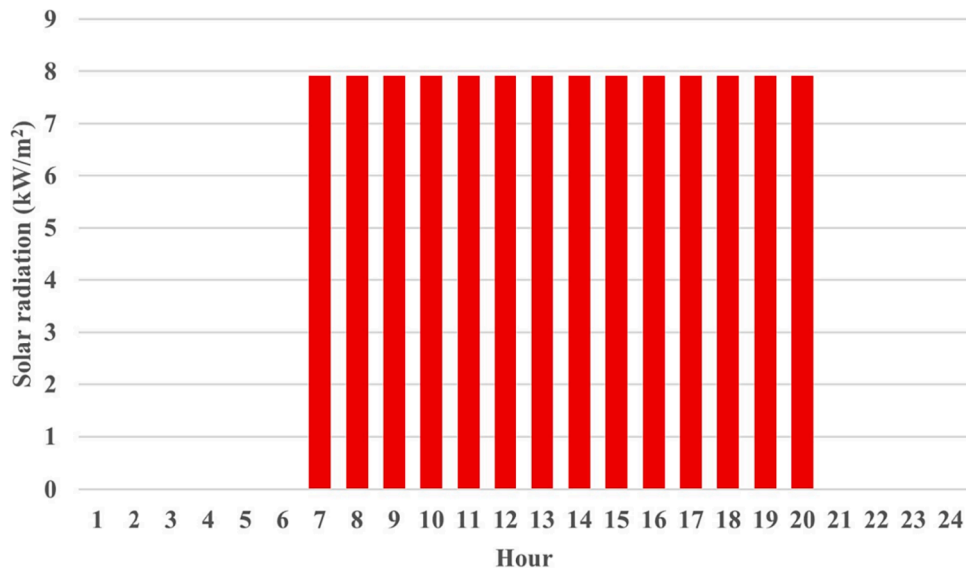


Fig. 6. The solar radiation in the simulation area [31].

3. Simulation

3.1. Simulation settings

The simulation is performed on the modified IEEE 123-bus feeder. The equipment and resources connected to each bus in this feeder are specified in Fig. 3.

Table 2 shows the type of resources or equipment, the bus number to which they are connected, and their capacity.

Other details of the IEEE 123 bus feeder are specified according to

Table 3

The Coefficients in the Gross Surplus Functions.

$a(i, AC) = 3.45$	$a(i, PHEV) = 0.002$	$a(i, W) = 0.002$	$a(i, L) = 0.76$	$a(i, Ent) = 0.3$
$b(i, AC) = 0.06$	$b(i, PHEV) = 0.37$	$b(i, W) = 0.466$	$b(i, L) = 0.06$	$b(i, Ent) = 0.06$

Table 4

The Parameters of Household Appliances.

Preferred household temperature (Celsius)				
$TempComf(i) = 23.89^\circ$	$TempComf \min(i) = 21.11^\circ$		$TempComf \max(i) = 25^\circ$	
AC (54000 BTU, an energy efficiency ratio of 12.75)				
$\Delta(i) = 0.9$	$\nabla(i) = -0.0045$		$P \max(i, 'AC') = 4.235(kW)$	
PHEV				
$EffPHEV(i) = 95\%$		$Capacity = 12(kWh)$		
$P \max(i, 'PHEV') = 3.7(kW)$	$E \min PHEV(i) = 9.88(kWh)$		$E \max PHEV(i) = 10.4(kWh)$	
Washer-dryer (1500 RPM, 8.5 kg)				
$P \max(i, 'W') = 2.2(kW)$	$E \min W(i) = 5.3(kWh)$		$E \max W(i) = 5.44(kWh)$	
Controllable LED lights (45 W LED, 5800 lumens)				
$P \max(i, 'L') = 0.58(kW)$		$PLightComf(i) = 0.435(kW)$		
Entertainment System				
TV (85" QLED 8K UHD HDR Smart TV)				
$avg. power = 255(W)$		$max. power = 585(W)$		
5.1-Channel Home Theater System				
$avg. power = 275(W)$		$max. power = 580(W)$		
Game Console				
$avg. power = 158.2(W)$		$max. power = 310(W)$		
Personal Computer				
$avg. power = 185(W)$		$max. power = 295(W)$		
$P \max(i, 'Ent') = 1.77(kW)$				
HESS				
$\sigma_1 = 23 \times 10^{-8}$	$\sigma_2 = 7 \times 10^{-8}$	$\sigma_3 = 25 \times 10^{-8}$	$\sigma_4 = 0.233$	$\gamma(i) = 0.2$
$PHEssD \max(i) = -5(kW)$	$PHEssC \max(i) = 5(kW)$	$CapHEss(i) = 13.5(kWh)$	$EffHEss(i) = 90\%$	

Table 5
The Consumers' Desired Time of Using ENT.

	Household category	Active hours	Standby hours	Off hours
TV	1	10 → 12, 18 → 20, 21 → 24	8 → 10, 12 → 18, 20 → 21	0 → 8
	2	19 → 20, 21 → 24	18 → 19, 20 → 21	0 → 18
Home Theater	1	10 → 12, 18 → 20, 21 → 24	8 → 10, 12 → 18, 20 → 21	0 → 8
	2	19 → 20, 21 → 24	18 → 19, 20 → 21	0 → 18
Game Console	1	18 → 20	8 → 18, 20 → 24	0 → 8
	2	19 → 20	18 → 19, 20 → 24	0 → 18
Personal Computer	1	8 → 12, 13 → 15	–	0 → 8, 12 → 13, 15 → 24
	2	18 → 19	–	0 → 18, 19 → 24

Table 6
The Consumers' Desired Power Consumption of ENT.

First category	t: 9, 10, 14, 15 0.1859 (kW)	t: 22, 23, 24 0.5302 (kW)	t: 13, 16, 17, 18, 21 0.0009 (kW)	t: 19, 20 0.6882 (kW)	t: 11, 12 0.7152 (kW)
Second category	t: 19 0.1859 (kW)	t: 22, 23, 24 0.5302 (kW)	t: 21 0.0009 (kW)	t: 20 0.6882 (kW)	

Table 7
Parameters in Simulation.

$\max CES(b) = \max DES(b) = 0.5 \times CapES(b)$	$\zeta = 1 \times 10^{-14}$
$\max QWT(b) = 0.659$	$\max QMT(b) = 0.75$

Table 8
The Desired Set of Times for Consumers' Appliances.

Household Category	1	2
$Tm(i, AC)$	{8, 9, ..., 24}	{17, 18, ..., 24}
$Tm(i, PHEV)$	{1, 2, ..., 8, 20, 21, ..., 24}	{1, 2, ..., 8, 20, 21, ..., 24}
$Tm(i, W)$	{8, 9, ..., 24}	{18, 19, ..., 24}
$Tm(i, L)$	{19, 20, ..., 24}	{19, 20, ..., 24}
$Tm(i, Ent)$	{8, 9, ..., 24}	{18, 19, ..., 24}

[28]. All loads of the system are household consumers divided into two parts. Households in the first category are at home all day, while the second category is not at home between 8:00–18:00. The simulation is done in an area in California on a typical summer day. According to the statistics and growth rate in the tested area, the number of people in each household is considered 6 [13]. The temperature, wind speed, and solar radiation are shown in Fig. 4, Fig. 5, and Fig. 5, respectively (Fig. 6).

It was assumed that the air conditioning system was determined as the first rank of the consumers' priority list based on the fact that the simulation was run for a typical summer day. Then, the PHEV and washing-drying machine were chosen as the second and third ranks of the list. Finally, the last priorities were the lighting system and the entertainment system. Therefore, the coefficients used in gross surplus functions of consumers' household appliances are shown in Table 3.

The consumers can adjust these parameters according to their desired comfort level and preferences to reach the optimal balance between cost, gross surplus, and comfort level. Table 4 shows the information related to the simulation of household appliances and HESSs. The desired times of using the entertainment devices of the consumers are shown in Table 5. Table 6 shows $PEntComf(i, t)$ for each category of consumers. Table 7 shows the maximum charge and discharge power of ESSs, constant step size in DRPHESs, and the coefficients of the

Table 9
The Parameters in Spinning Reserve.

$\lambda = 3$ (Failure per year)
Time to start up micro turbines = 10min
Acceptable system's risk = 0.001

maximum reactive power produced by WTs and MTs.

The coefficients of the maximum reactive power produced are the tangent of the inverse cosine of the power factor. The power factor is considered 0.835 for WT and 0.8 for MT. Table 8 shows the set of times that the first and second categories of households want to use their home appliances.

The parameters used in determining the spinning reserve of the system are shown in Table 9. Table 10 shows the coefficients and fixed numbers used in the utility cost function.

The parameters in the cost function are determined so that the energy price in the wholesale market and the price of selling energy to household consumers in this simulation will be the same as the prices reported in reality in the simulation area [32–34]. Table 11 shows the price of active and reactive power purchased from microturbines. The parameters used in the generation of the wind and solar resources scenarios are shown in Table 12.

3.2. Simulation results

The simulation in this paper is implemented in two general modes: 1. without the application of DRPHESs; and 2. with the application of DRPHESs. Then, in each of the two general modes, the simulation has been implemented in 1. Normal operation mode and 2. Emergency operation mode. The simulation was carried out using GAMS optimization software version 25.1.3 and MATLAB on a computer system with Intel Core i7-5500 U CPU @ 2.40 GHz 2.40 GHz processor and 8 GB of memory. The simulation time for normal operation mode was about 9.5 s, and the average simulation time for emergency operation mode was about 1.313 s.

Table 10
The Parameters in the Utility Company's Cost Function.

$k = 3$		
$cc_{11} = 0.000200(\$/kWh)^2$	$cc_{12} = 0.2(\$/kWh)$	$cc_{13} = 130000(\$)$
$cc_{21} = 0.000200(\$/kWh)^2$	$cc_{22} = 0.5(\$/kWh)$	$cc_{23} = 150000(\$)$
$cc_{31} = 0.000202(\$/kWh)^2$	$cc_{32} = 0.2(\$/kWh)$	$cc_{33} = 170000(\$)$
$X_1 = 733.3(kWh)$	$X_2 = 1133.3(kWh)$	$X_3 = 1666.6(kWh)$

Table 11

The Energy Price of MTs.

$MTP(t) = 174.35(\$/MWh), \forall t = \{1, 2, 3, \dots, 24\}$ [35]
$MTQ(t) = 2.40(\$/MVAh), \forall t = \{1, 2, 3, \dots, 24\}$ [36,37]

Table 12

The Parameters in Scenario Generation.

$r_1 = 0.1$	$r_2 = 0.38$	$r_3 = 0.02$	$v_{ci} = 2(m/s)$	$v_1 = 4(m/s)$
$v_2 = 6(m/s)$	$v_r = 8(m/s)$	$v_{co} = 10(m/s)$	$R_c = 10(kW/m^2)$	$Ra_1 = 5.5(kW/m^2)$

3.2.1. The mode without applying DRPHESs

In this stage of the simulation, the objective function of SHEMSs is to maximize the gross surplus of each consumer, and the DRP algorithm (40), (41), and (42) are not applied. All of the constraints related to HESSs are also omitted. In other words, every consumer maximizes their net surplus regardless of the prices set by the utility company and without using their HESS. The simulation of this stage takes 9.422 s. Fig. 7 and Fig. 8 show the household appliances' energy consumption of

a typical consumer of the first and second categories, respectively. Fig. 9 also shows the energy consumption of all consumers for each hour.

As shown in Fig. 7, since the simulation is on a typical day in the summer, a massive share of the demand belongs to the AC. In addition, although the consumer is at home all day, the car is not charged during the day hours. It makes the car available during the day and thus increases the consumer's convenience.

As mentioned, consumers of the second category are not at home during the day. Therefore, according to Fig. 8, the energy consumption of this consumer is zero between 8:00 and 16:00. The consumer is not at home until 18:00. However, the AC of this consumer is turned on 2 h before the consumer enters the house. Hence, the inside temperature of the house is pleasant when the consumer enters, which increases the consumer's comfort level.

According to Fig. 9, the energy consumption diagram of all

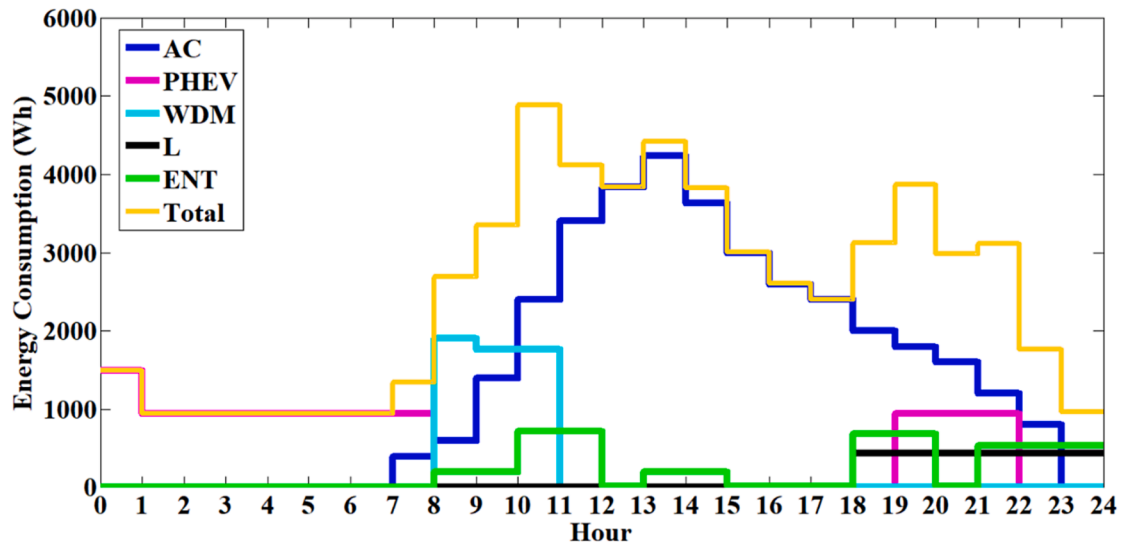


Fig. 7. The energy consumption of a typical consumer of the first category without applying DRPHESs.

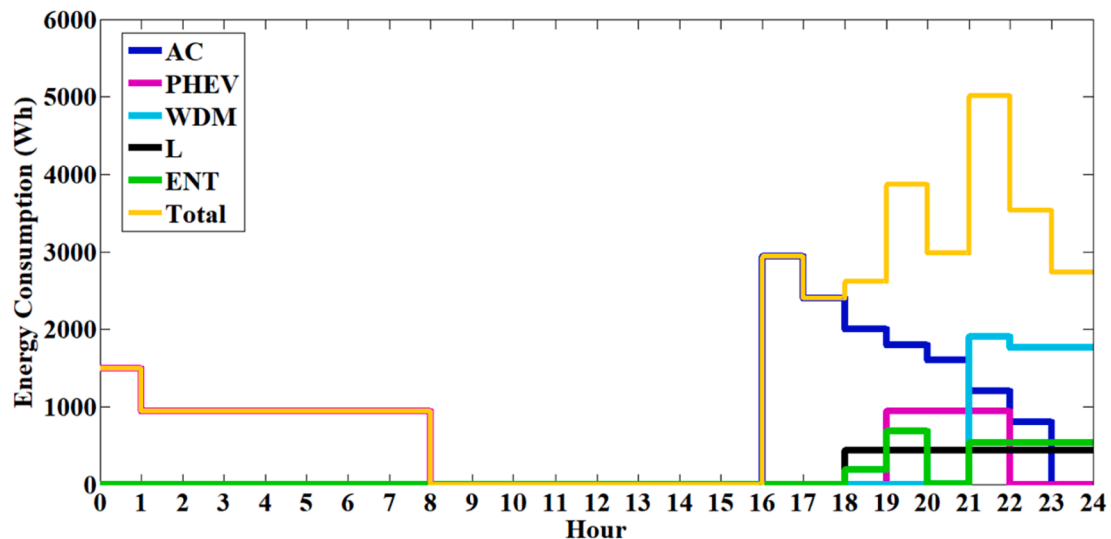


Fig. 8. The energy consumption of a typical consumer of the second category without applying DRPHESs.

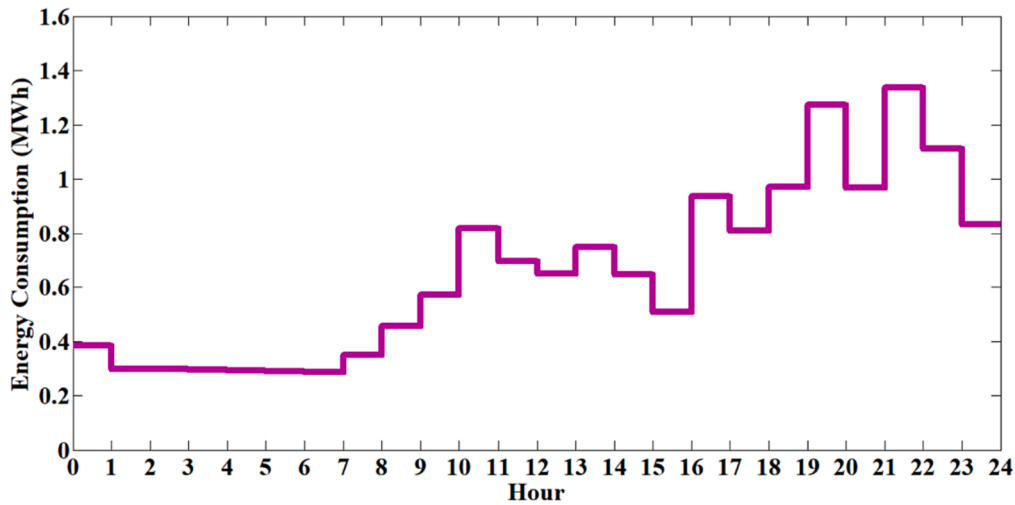


Fig. 9. The energy consumption of all consumers without applying DRPHESs.

Table 13

The Energy Prices in the Wholesale Market without Applying DRPHESs.

$UPBP(t) = UPSP(t)(\$/MWh)$								
t1: 75.771	t2: 75.596	t3: 75.594	t4: 75.589	t5: 75.585	t6: 75.580	t7: 75.575	t8: 75.702	t9: 75.914
t10: 76.142	t11: 89.095	t12: 76.391	t13: 76.297	t14: 88.736	t15: 76.292	t16: 76.014	t17: 89.683	t18: 89.057
t19: 89.854	t20: 122.547	t21: 89.844	t22: 122.672	t23: 90.558	t24: 89.163			

Table 14

The Energy Prices in The Retail Market without Applying DRPHESs.

$CP(t)(\$/kWh)$							
t1: 11.761	t2: 9.139	t3: 9.113	t4: 9.030	t5: 8.968	t6: 8.906	t7: 8.819	t8: 10.725
t9: 13.905	t10: 17.328	t11: 25.068	t12: 21.064	t13: 19.654	t14: 22.914	t15: 19.578	t16: 15.415
t17: 28.598	t18: 24.841	t19: 29.623	t20: 38.778	t21: 29.562	t22: 40.676	t23: 33.849	t24: 25.475

Table 15

Simulation Results in Normal Operation Mode without Applying DRPHESs.

Load factor	0.494
Peak demand (kWh)	1335.859
Total demand (kWh)	15836.211
Minimum voltage in the network (p.u.)	0.958
Maximum voltage in the network (p.u.)	1.033
Maximum line load (kW)	10.000
Consumer's payment (\$)	3928.204
Cost of buying energy from the upstream network (\$)	659.959
Cost of buying energy from MTs (\$)	0
Income from selling energy to the upstream network (\$)	307.342
The revenue of utility company (\$)	4235.546
The profit of utility company (\$)	3575.587
Consumers' gross surplus (\$)	27030.153
Consumers' net surplus (\$)	23101.949
Social welfare (\$)	26677.536
Simulation time (seconds)	2.328

consumers has a peak load between 10 and 11 and a peak load between 21 and 22. Considering that, the simulation is on a typical summer day, we can expect that the energy consumption of the system is higher during the noon peak than the night peak. However, since half of the households are not at home from 8:00 to 18:00, the most energy consumption is related to the night peak.

According to the demand, energy prices in the wholesale and retail markets are shown in Tables 13 and 14, respectively. The prices obtained from the SHEMS optimization program are placed in the objective function of the SHSRID in the parameters $UPBP(t)$, $UPSP(t)$, and $CP(t)$.

Table 16

Location of Faulted Resources and Equipment in each Emergency Case without Applying DRPHESs.

	Faulted MT on [bus]	Faulted Line between buses [bus, bus]	Faulted WT on [bus]	Faulted PV on [bus]	Faulted ESS on [bus]	Faulted SVC on [bus]
EC1	-	[60,67]	-	-	-	-
EC2	[67], [1 0 1]	[60,67], [101,105]	-	-	-	-
EC3	-	[18,35], [60,67]	-	-	-	-
EC4	[48], [67], [1 0 1]	[18,35], [35,40], [60,67], [101,105]	-	-	-	-
EC5	[48], [67], [76], [87]	[18,35], [35,40], [60,67], [101,105]	[39], [46]	[75], [95]	[38], [70], [84], [1 0 9]	[44], [81], [87], [89]
EC6	[48], [67], [76], [81], [87], [93], [1 0 1]	[18,35], [35,40], [60,67], [101,105], [103,104]	[39], [46], [82], [86], [1 1 2]	[75], [95], [1 0 6]	[38], [70], [84], [90], [1 0 9]	[44], [81], [87], [89], n

3.2.1.1. Normal operation mode. As explained in the system model section, ISO optimizes the active and reactive output power of the system's resources and equipment according to the information about the

Table 17
Technical Information in each Emergency Case without Applying DRPHESs.

Emergency Cases	EC1	EC2	EC3	EC4	EC5	EC6
Number of microgrids	11	9	16	14	9	4
Number of faults	1	4	2	7	20	30
Number of consumers in faulted area	140	140	214	214	214	214
Percentage of interrupted loads	41.42	41.42	63.31	63.31	63.31	63.31
Percentage of active power loss	0	12.74	0	11.35	42.22	58.91
Percentage of reactive power loss	0	14.34	0	12.71	38.15	57.86
Number of interrupted consumers	0	0	0	0	12	94
Percentage of interrupted consumers	0	0	0	0	5.61	43.93
Active demand not supplied (kWh)	0	0	0	0	44.972	344.398
Total active demand	1482.001	1482.001	2265.337	2265.337	2265.337	2265.337
Percentage of active demand not supplied	0	0	0	0	1.99	15.20
Reactive demand not supplied (kVarh)	0	0	0	0	26.983	206.639
Total reactive demand	889.201	889.201	1359.202	1359.202	1359.202	1359.202
Percentage of reactive demand not supplied	0	0	0	0	1.99	15.20
Generators for regulating Voltage and controlling frequency in each isolated part of the faulted area (Slack Bus)	67	76, 108	35, 67	35, 44, 76, 108	35, 49, 101, 108	35, 44, 78, 108

Table 18
Economic and Security Information in each Emergency Case without Applying DRPHESs.

Emergency Cases	EC1	EC2	EC3	EC4	EC5	EC6
Peak demand (kWh)	553.501	553.501	845.692	845.692	814.030	719.125
Total demand (kWh)	1482.001	1482.001	2265.337	2265.337	2220.446	1920.939
Load factor	0.89	0.89	0.89	0.89	0.88	0.89
Minimum voltage in the network (p.u.)	0.998	0.999	0.998	0.999	0.998	0.996
Maximum voltage in the network (p.u.)	1.001	1.001	1.001	1.001	1.001	1.003
Maximum line load (kW)	0.475	0.475	0.552	0.790	1.185	1.646
Consumer's payment (\$)	548.086	548.086	837.803	837.803	820.294	710.866
Cost of buying energy from MTs (\$)	166.780	155.728	263.350	220.824	295.449	246.715
The revenue of utility company (\$)	548.086	548.086	837.803	837.803	820.294	710.866
The profit of utility company (\$)	381.306	392.358	574.453	616.979	524.845	464.151
Consumers' gross surplus (\$)	4923.240	4923.240	7525.524	7525.524	7103.532	4219.920
Consumers' net surplus (\$)	4375.154	4375.154	6687.721	6687.721	6283.238	3509.054
Social welfare (\$)	4756.460	4767.512	7262.174	7304.700	6808.083	3973.205
Simulation time (seconds)	0.812	1.047	1.218	1.078	1.360	0.422

Table 19
Economic and Security Information in the Connected Part of the DN to the Upstream Network without Applying DRPHESs.

Emergency Cases	EC1, EC2	EC3, EC4, EC5, EC6
Peak demand (kWh)	782.358	490.167
Total demand (kWh)	2096.262	1312.926
Load factor	0.89	0.89
Minimum Voltage in the network (p.u.)	0.982	0.989
Maximum Voltage in the network (p.u.)	1.006	1.002
Maximum line load (kW)	1.897	2.101
Consumer's payment (\$)	775.265	485.549
Cost of buying energy from the upstream network (\$)	93.678	64.789
Cost of buying energy from MTs (\$)	0	15.677
Income from selling energy to the upstream network (\$)	4.098	0.534
The revenue of utility company (\$)	779.363	486.083
The profit of utility company (\$)	685.685	405.617
Consumers' gross surplus (\$)	6962.868	4360.584
Consumers' net surplus (\$)	6187.603	3875.035
Social welfare (\$)	6873.288	4280.652
Simulation time (seconds)	0.375	0.328

consumers, equipment, and resources. Table 15 shows the results of the simulation in the normal operation mode.

3.2.1.2. Emergency operation mode. In this stage, faults have occurred in the network, which causes the outage of resources, equipment, lines, or all three. According to the U.S. Energy Information Administration (EIA), the SAIDI for the simulation area in 2021 is estimated to be

between 2 and 3 h. In this paper, the interruption hours for reconnecting the isolated part to the upstream network are 3 h, considering the worst scenarios [38]. According to Fig. 9, the highest energy consumption of the network is between 19:00 and 22:00. The emergency occurs in these three hours to model the most destructive modes in the simulation. Six emergency cases simulate the emergency operation mode: 1. EC1, 2. EC2, 3. EC3, 4. EC4, 5. EC5, and 6. EC6. Table 16 shows faulted resources, equipment, and lines in each case.

Fig. 15A shows microgrid formation in the DN topology for each emergency case without applying DRPHESs. Table 17 indicates the technical information related to the emergency cases.

Clearly, without applying the SHSRDE, 41.42 % of the network loads in EC1 and EC2 and 63.31 % of the network loads in cases EC3, EC4, EC5, and EC6 are interrupted. Therefore, the restored load of the system is equal to zero in all cases. As a result, system resiliency is zero. Table 17 shows that using the SHSRDE in EC1 to EC4, despite the faults, prevents the interruption of network loads in the isolated part of the network by converting the DN into several self-sufficient microgrids.

However, major destructive disasters have devastating effects on a DN. Interrupted loads caused by them are much more difficult to restore than a typical outage. Therefore, to consider these destructive disasters in the simulation of this paper, the proposed model has been evaluated in EC5 and EC6. In EC5 and EC6, the shortage of resources and equipment and the weak DN caused the interruption in a large number of consumers. After applying the SHSRDE, the amount of system load restored by converting the network into several self-sufficient microgrids is 100 % in EC1 to EC4, 98.02 % in case EC5, and 98.02 % in EC6. Therefore, the resiliency of the system reaches 0.9533. This number shows that the application of the SHSRDE successfully restores the

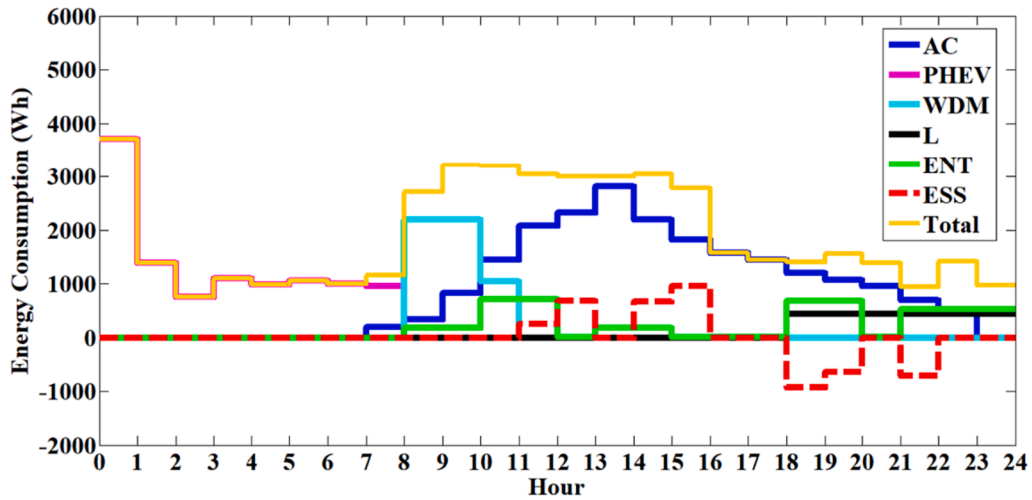


Fig. 10. The energy consumption of a typical consumer of the first category with applying DRPHESs.

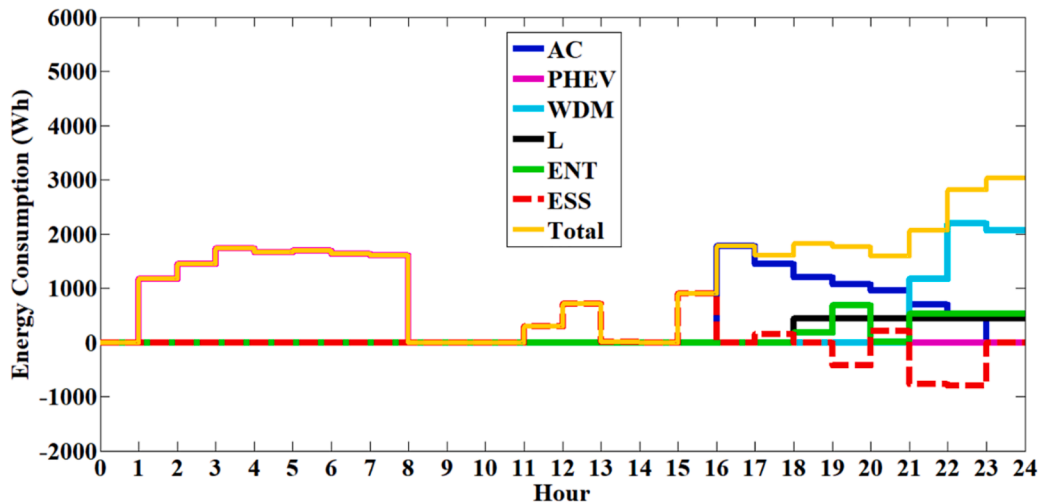


Fig. 11. The energy consumption of a typical consumer of the second category with applying DRPHESs.

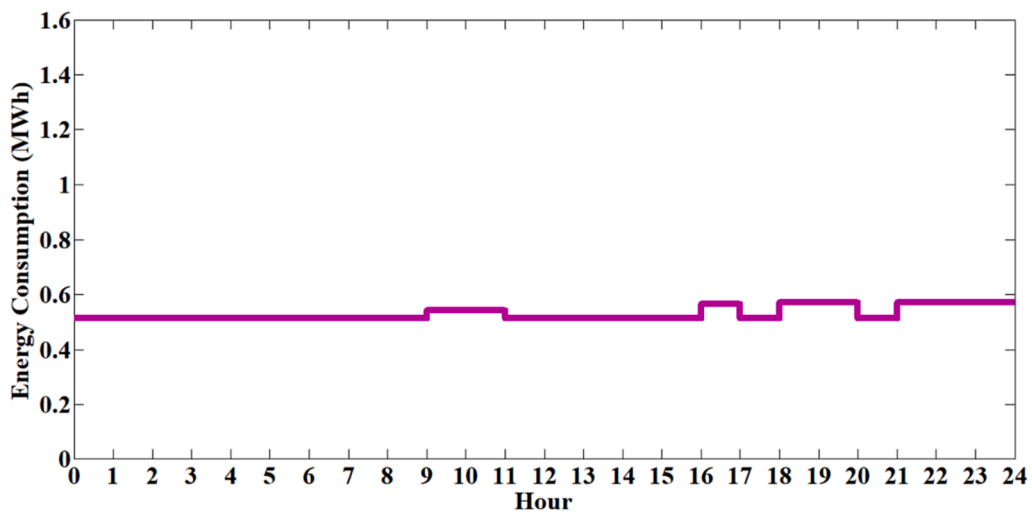


Fig. 12. The energy consumption of all consumers with applying DRPHESs.

system loads 95.33% of the time immediately during emergency operation conditions and continues to supply these loads for 3 h. Table 18 shows the economic and security information in each of the six

emergency cases in the isolated part of the network.

Since the destructive event in EC2 is more severe than in EC1, the cost of purchasing energy from MTs in EC2 is expected to be higher.

Table 20
The Energy Prices in The Wholesale Market by Applying DRPHESs.

$UPBP(t) = UPSP(t)(\$/MWh)$							
t1: 76.028	t2: 76.028	t3: 76.028	t4: 76.028	t5: 76.028	t6: 76.028	t7: 76.028	t8: 76.028
t9: 76.028	t10: 76.085	t11: 76.085	t12: 76.028	t13: 76.028	t14: 76.028	t15: 76.028	t16: 76.028
t17: 76.133	t18: 76.028	t19: 76.143	t20: 76.143	t21: 76.028	t22: 76.143	t23: 76.143	t24: 76.143

Table 21
The Energy Prices in The Retail Market by Applying DRPHESs.

$CP(t)(\$/kWh)$							
t1: 15.608	t2: 15.608	t3: 15.608	t4: 15.608	t5: 15.608	t6: 15.608	t7: 15.608	t8: 15.608
t9: 15.608	t10: 16.467	t11: 16.467	t12: 15.609	t13: 15.608	t14: 15.609	t15: 15.608	t16: 15.607
t17: 17.179	t18: 15.609	t19: 17.334	t20: 17.334	t21: 15.609	t22: 17.334	t23: 17.334	t24: 17.334

Table 22
Simulation Results in Normal Operation Mode by Applying DRPHESs.

Load factor	0.926
Peak demand (kWh)	572.374
Total demand (kWh)	12714.608
Minimum voltage in the network (p.u.)	0.966
Maximum voltage in the network (p.u.)	1.032
Maximum line load (kW)	5.553
Consumer's payment (\$)	2051.903
Cost of buying energy from the upstream network (\$)	528.716
Cost of buying energy from MTs (\$)	0
Income from selling energy to the upstream network (\$)	446.997
The revenue of utility company (\$)	2411.094
The profit of utility company (\$)	1970.184
Consumers' gross surplus (\$)*	27029.942
Consumers' net surplus (\$)	24978.039
Social welfare (\$)	26948.223
Simulation time (seconds)	2.360

* In the mode of applying DRPHESs, in all the tables related to the economic results, the operating cost of HESSs is also included in the consumers' gross surplus.

However, with a detailed examination, we find that despite the equal load, the energy produced by the MTs in EC1 is 949.813 kWh, and in EC2 is 889.188 kWh. As a result, the share of power generation by MTs compared to ESSs, WTs, and PVs in EC1 is higher than in EC2. Consequently, the security and resiliency of the DN are higher in EC1 than in EC2. \$11,052 difference in the cost of energy generation in these two cases is the cost of achieving more network resiliency and security. Similarly, despite the more destructive event in EC4 and equal load in these two cases, the power generation of MTs in EC3 is 1501.010 kWh, and in EC4 is 1262.355 kWh. As a result, the energy generation cost in

Table 23
Technical Information in each Emergency Case by Applying DRPHESs.

Emergency Cases	EC1	EC2	EC3	EC4	EC5	EC6
Number of microgrids	11	10	16	14	10	7
Number of faults	1	4	2	7	20	30
Number of consumers in faulted area	140	140	214	214	214	214
Percentage of interrupted loads	41.42	41.42	63.31	63.31	63.31	63.31
Percentage of active power loss	0	12.74	0	11.35	42.22	58.91
Percentage of reactive power loss	0	14.34	0	12.71	38.15	57.86
Number of interrupted consumers	0	0	0	0	0	4
Percentage of interrupted consumers	0	0	0	0	0	1.87
Active demand not supplied (kWh)	0	0	0	0	0	19.714
Total active demand	687.409	687.409	1049.604	1049.604	1049.604	1049.604
Percentage of active demand not supplied	0	0	0	0	0	1.88
Reactive demand not supplied (kVarh)	0	0	0	0	0	11.828
Total reactive demand	412.445	412.445	629.762	629.762	629.762	629.762
Percentage of reactive demand not supplied	0	0	0	0	0	1.88
Generators for regulating Voltage and controlling frequency in each isolated part of the faulted area (Slack Bus)	67	76, 108	35, 67	35, 44, 76, 108	35, 49, 101, 108	35, 44, 78, 108

EC3 is higher than in EC4 by \$42,526. By comparing the optimal response in these two cases, we find that the number of microgrids in EC3 is more, which increases security and resiliency, and this amount of additional cost is the cost of providing more security and resiliency.

In contrast to EC1 to EC4, the power supply is interrupted to 12 consumers in EC5. This causes a decrease of 5.61 % in the gross surplus of consumers and 6.80 % in social welfare. However, in EC6, because the power supply is interrupted to 94 consumers, consumers' gross surplus is reduced by 43.93 % compared to EC4. Social welfare also decreased by 45.61 %.

Another significant point obtained from Table 18 is that with the increase in the number of interrupted consumers, in addition to the gross surplus of consumers and social welfare, the revenue and profit of the utility company also decrease. One of the advantages of the proposed model is that the interests of consumers and ISO, who seek to increase their surplus and comfort and increase the security and resiliency of the system, respectively, are aligned with the interests of the utility company, which is a private organization, seeks to maximize its profit. In other words, none of the players (from an economic point of view) in this system will benefit from the loss of another.

Table 19 shows the economic and security information related to the connected part of the DN to the upstream network in emergency operation mode without applying DRPHESs.

In confirmation of the previous point, as it is clear from Tables 18 and 19, as the number of faults increases and more consumers are interrupted in the faulted area, the total profit of the utility company and the net surplus of all consumers (from both the faulted area and the area connected to the upstream network) are decreased. As a result, social welfare (resulting from both of the areas) also decreases.

Table 24
Economic and Security Information in each Emergency Case by Applying DRPHESs.

Emergency Cases	EC1	EC2	EC3	EC4	EC5	EC6
Peak demand (kWh)	237.271	237.271	362.193	362.193	362.193	355.386
Total demand (kWh)	687.409	687.409	1049.604	1049.604	1049.604	1029.890
Load factor	0.97	0.97	0.97	0.97	0.97	0.97
Minimum voltage in the network (p.u.)	0.999	1.000	0.999	0.998	0.999	0.999
Maximum voltage in the network (p.u.)	1.000	1.000	1.000	1.001	1.001	1.001
Maximum line load (kW)	0.301	0.204	0.204	0.952	0.636	0.880
Consumer's payment (\$)	115.477	115.477	176.318	176.318	176.318	173.006
Cost of buying energy from MTs (\$)	66.066	59.074	134.980	111.490	139.447	144.757
The revenue of utility company (\$)	115.477	115.477	176.318	176.318	176.318	173.006
The profit of utility company (\$)	49.411	56.403	41.338	64.828	36.871	28.249
Consumers' gross surplus (\$)	4921.283	4921.283	7518.656	7518.656	7518.656	7308.217
Consumers' net surplus (\$)	4805.806	4805.806	7342.338	7342.338	7342.338	7135.211
Social welfare (\$)	4855.217	4862.209	7383.676	7407.166	7379.209	7163.460
Simulation time (seconds)	1.000	1.406	1.656	1.328	1.750	1.422

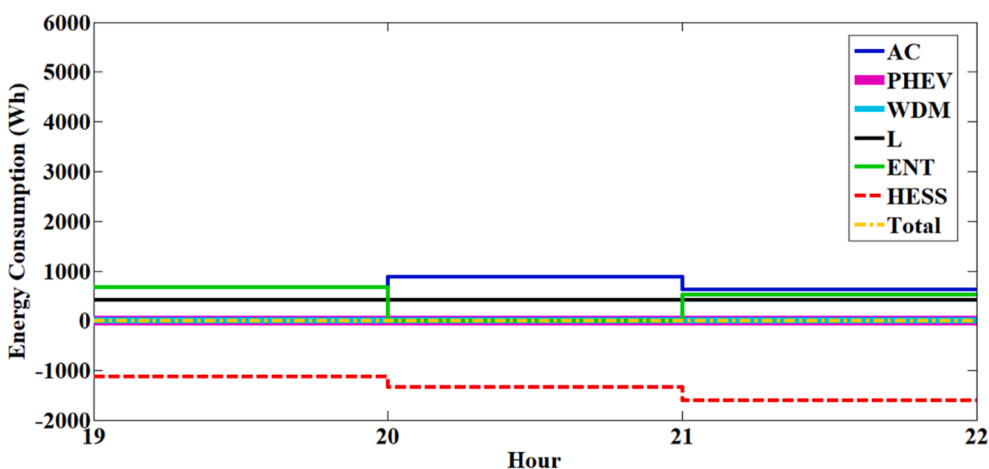


Fig. 13. The energy consumption of an interrupted consumer of the first category in EC6 by applying DRPHESs.

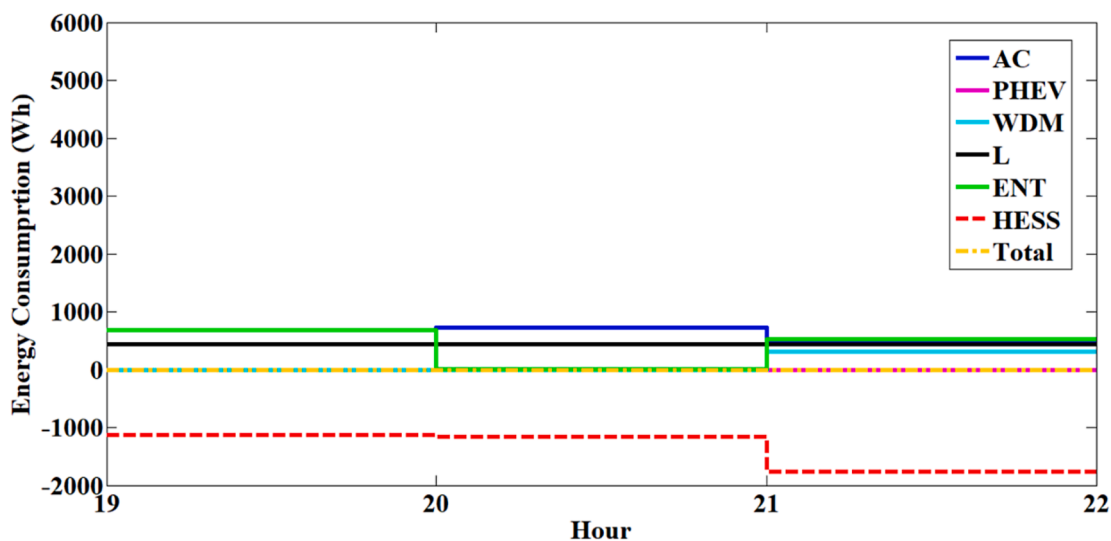


Fig. 14. The energy consumption of an interrupted consumer of the second category in EC6 with applying DRPHESs.

3.2.2. The mode with applying DRPHESs

The objective function of DRPIHESs is to maximize the net surplus of each consumer in this stage. The DRP uses an RTP algorithm and HESSs to optimize consumers' power consumption. The simulation of this stage takes 7.218 s. Fig. 10 shows the energy consumption of household appliances of a typical consumer of the first category.

At this stage, by using DRPHESs, the consumers achieve a trade-off between their convenience and net surplus and the amount of money they pay for their energy consumption. Considering the trade-off, as shown in Fig. 10, significantly reduces the energy consumption of the AC compared to Fig. 7. In other words, for example, by accepting a slight increase in the temperature inside the house (so that the temperature

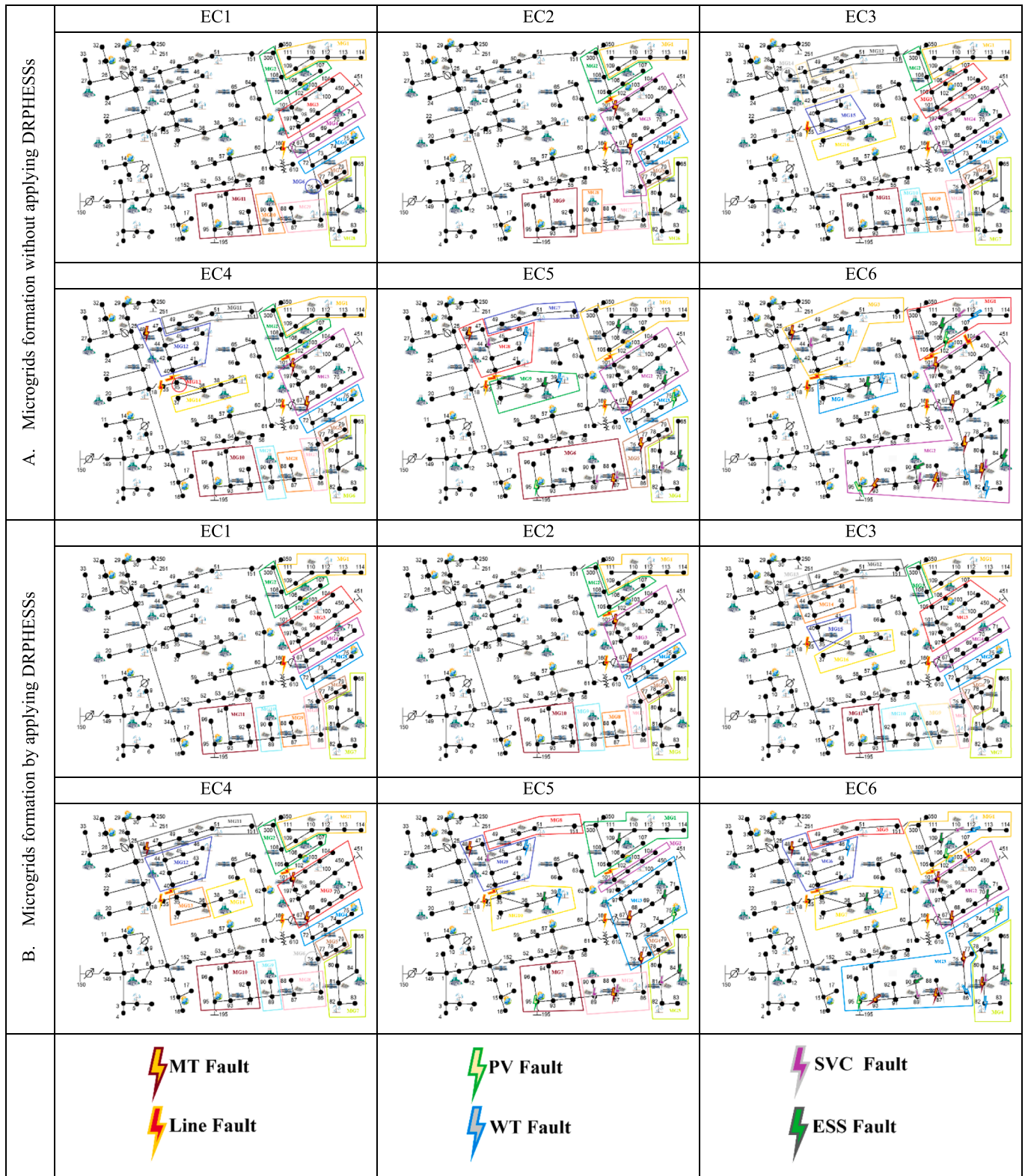


Fig. 15. Microgrids formation in The DN topology for the mode A. without applying DRPHESSES, and B. with applying DRPHESSES.

inside the house is still within the desired range of the consumer) between 13:00–14:00, the energy consumption of the AC decreases by 1417.15 Wh. In addition, HESSs integrated with the DRP reduce consumption during peak hours by charging during low-demand hours and discharging during high-demand hours.

Fig. 11 shows the energy consumption of household appliances of a

typical consumer of the second category. According to Fig. 11, the HESS is in charging mode when the consumer is not home. Thus, the HESS provides some of the energy needed by the consumer during peak hours of the network when the energy price is high. Fig. 12 shows the energy consumption of all consumers for each hour. Fig. 12 shows that utilizing the RTP program in DRPHESSES flattens the energy consumption graph of

Table 25
Economic and Security Information in the Connected Part of the DN to the Upstream Network by Applying DRPHESs.

Emergency Cases	EC1, EC2	EC3, EC4, EC5, EC6
Peak demand (kWh)	334.732	209.810
Total demand (kWh)	970.236	608.041
Load factor	0.97	0.97
Minimum Voltage in the network (p.u.)	0.989	0.993
Maximum Voltage in the network (p.u.)	1.012	1.007
Maximum line load (kW)	3.209	0.946
Consumer's payment (\$)	162.984	102.143
Cost of buying energy from the upstream network (\$)	40.780	20.949
Cost of buying energy from MTs (\$)	0	0
Income from selling energy to the upstream network (\$)	42.469	18.883
The revenue of utility company (\$)	205.453	121.026
The profit of utility company (\$)	164.673	100.077
Consumers' gross surplus (\$)	6957.413	4359.218
Consumers' net surplus (\$)	6794.429	4257.075
Social welfare (\$)	6959.102	4357.152
Simulation time (seconds)	0.343	0.203

total consumers compared to Fig. 9.

According to the demand, energy prices in the wholesale and retail markets are shown in Tables 20 and 21, respectively. The prices obtained from the DRPHESs are placed in the objective function of the SHSRDE in the parameters $UPBP(t)$, $UPSP(t)$, and $CP(t)$.

By comparing Tables 13 and 14 to Tables 20 and 21, the RTP algorithm reflects the energy price in the wholesale market to the retail market and home consumers. Therefore, it encourages consumers to adjust their consumption according to the wholesale market price. Because of the modification of the consumers' consumption pattern, the average wholesale price and the average retail price of energy decreased by 9.78 % and 19.94 %, respectively.

3.2.2.1. Normal operation mode. Table 22 shows the simulation results in the normal operation mode.

By applying DRPHESs, each consumer saves approximately 5.55\$ per day. This fact shows that even if there is no cost for operating HESSs, the initial cost of purchasing each HESS will break even within an approximate period of 4.9 years (the approximate purchase cost of a HESS is \$10,000 according to Tesla Power Wall). Usually, the producers of these HESSs consider ten years of warranty for this product, which means that from the fifth year, consumers can use these batteries for five years with net profit without paying any costs. Comparing the mode without applying DRPHESs and with DRPHESs indicates that reflecting the wholesale market energy price to the retail market and home consumers and utilizing HESSs leads to a 57.15 % reduction in peak load, 87.45 % improvement in load factor, 0.84 % increase in minimum and 0.1 % reduction in maximum voltage, 47.77 % decrease in the consumers' payment to the utility company, 19.89 % reduction in the energy purchase cost and network operation, an increase of 8.12 % in net surplus of consumers and 1.01 % in social welfare, and 44.47 % reduction in lines load and congestion.

3.2.2.2. Emergency operation mode. Fig. 15B shows microgrid formation in the DN topology for each emergency case by applying DRPHESs. Table 23 shows the technical information related to each case.

Table 23 shows that the simultaneous use of SHSRDE and DRPHESs successfully prevents the interruption of network loads in the faulted area isolated from the upstream network in EC1, EC2, EC3, EC4, and EC5. Comparing Tables 23 and 17 indicates that the proposed system significantly increases the ability of the system to restore loads so that in EC1 to EC5, the restored loads are 100 %, and in EC6 it reaches 98.12 %, and as a result, improves the resiliency to 0.9948. In other words, the simultaneous use of SHSRDE and DRPHESs can restore the loads

99.48 % of the time in case of multiple high-severity faults in emergency operation conditions.

In addition, the proposed model supplies the loads for 3 h until resolving technical problems and re-establishing the connection of the isolated part to the upstream network. It is done by transforming the network into several self-sufficient microgrids and reflecting the energy price in the wholesale market to the retail market. Table 24 shows the economic and security information related to each of the six emergency cases by applying DRPHESs for the isolated area.

Unlike EC1 to EC5, the power supply to 4 consumers is interrupted in EC6. This reduces 2.80 % of the gross surplus of consumers, as well as 2.92 % of social welfare. Comparing Table 24 with Table 18 shows that the average peak load and total load are reduced by 55.78 % and 52.28 %, respectively. Because of the demand reduction, the average cost of purchasing energy from MTs and the average payment of consumers is reduced by 52.52 % and 78.32 %, respectively. The average minimum voltage increased by 0.1 %. The average maximum voltage decreased by 0.1 %. The average transfer load of the line with the most load and congestion in the peak hour has improved by 38.18 %. Consequently, the improvements in the consumers' consumption pattern, the voltage profile, and the load of lines enhance the ability of ISO to control and maintain the system's security.

The RTP algorithm improves the load curve so that the average power factor increases by 9.04 %. The average net surplus and average social welfare increased by 26.58 % and 15.97 %, respectively. The increase in these two parameters in EC5 and EC6 is much more impressive due to the proposed system's ability to restore more loads in contrast to the mode without applying DRPHESs.

Integrating HESSs with DRP enables consumers to use the stored energy to supply their electrical energy demand when multiple faults occur in the network. They can use their appliances even when the power supply from the DN is interrupted. In EC6, the power supply to 4 consumers is interrupted. The simulation time of emergency DRPHESs for these 4 consumers is 0.172 s. Fig. 13 shows the energy consumed by a consumer of the first category of these four consumers during the power supply interruption hours.

Fig. 14 shows the energy consumed by a consumer of the second category of these four consumers during the power supply interruption hours.

The proposed system is tested under severe events to evaluate the network's resiliency in this paper. In this regard, the SOCHES rate of each of these four consumers is considered 0.3 at the beginning of the power supply interruption. Therefore, the worst possible condition is modeled in the simulation to evaluate the proposed system's efficiency. Fig. 13 and Fig. 14 show that HESSs can supply consumers' energy demand during power supply interruption hours.

Comparing Fig. 13 and Fig. 14 with Fig. 10 and Fig. 11 shows that the proposed system gives considerable importance to the desired convenience of the consumers. In such a way, despite the great disaster in EC6 and considering the worst cases in the resiliency evaluation, the interrupted consumers use all the devices they used in normal operation mode. Also, their energy consumption has not decreased. As a result, these two items help consumers achieve their desired level of comfort in this dire condition.

Table 25 shows the economic and security information related to the connected part of the DN to the upstream network in emergency operation mode by applying DRPHESs.

Applying DRPHESs for the area connected to the upstream network reduces the average peak load by 57.21 %, decreases the average total demand by 53.71 %, improves the average load factor by 8.99 %, reduces the average cost of energy purchase and network operation by 7.67 %, increases the average net surplus of consumers and average social welfare by 9.83 % and 1.46 %, respectively.

4. Discussion of main achievements

In this section, a brief explanation of the main achievements of this article is provided to provide more help for qualitative evaluation and comparison with other articles.

1. The integration of HESSs with the DRP reduces consumption during peak hours by charging during low-demand hours and discharging during high-demand hours. Applying DRPHESs leads to a 57.15 % reduction in peak load and, an 87.45 % improvement in load factor in normal operation mode, which results in a 47.77 % decrease in the consumers' payment.
2. Utilizing the RTP algorithm reflects the energy price in the wholesale market to home consumers. Therefore, it encourages consumers to adjust their consumption according to the wholesale market price. Because of the modification of the consumers' consumption pattern, the average wholesale price and the average retail price of energy decreased by 9.78 % and 19.94 %, respectively.
3. Without applying the SHSRDE, 41.42 % of the network loads in EC1 and EC2 and 63.31 % of the network loads in cases EC3, EC4, EC5, and EC6 are interrupted. After applying the SHSRDE, the amount of system load restored by converting the network into several self-sufficient microgrids is 100 % in EC1 to EC4, 98.02 % in case EC5, and 98.02 % in EC6. The simultaneous use of SHSRDE and DRPHESs in emergency operation mode significantly increases the ability of the system to restore loads so that in EC1 to EC5, the restored loads are 100 %, and in EC6, they reach 98.12 %.
4. In addition to improving network resiliency, the application of the proposed framework simultaneously enhances the economic efficiency. In a way that the simultaneous use of SHSRDE and DRPHESs in emergency operation mode the average cost of purchasing energy from MTs and the average payment of consumers is reduced by 52.52 % and 78.32 %, respectively.
5. In addition to the faulted part of the DN, applying DRPHESs for the area connected to the upstream network reduces the average peak load by 57.21 %, decreases the average total demand by 53.71 %, improves the average load factor by 8.99 %, reduces the average cost of energy purchase and network operation by 7.67 %, increases the average net surplus of consumers and average social welfare by 9.83 % and 1.46 %, respectively.
6. The proposed system is tested under severe events to evaluate the network's resiliency: 1. The emergency occurs in the times with the highest energy consumption of the network. 2. 63.31 % of the network loads in EC6 are interrupted. 3. 58.91 % of active power and 57.86 % of reactive power of the resources are lost in EC6. 4. 30 faults have occurred in EC6. 5. The SOCHES rate of each of the four not supplied consumers is considered 0.3 at the beginning of the power supply interruption.
7. The DRPHESs is executed by considering consumers' comfort and priority settings. The proposed model does not implement load shedding through direct load control. The results show that the proposed system gives considerable importance to the desired convenience of the consumers. In such a way, despite the great disaster in EC6 and considering the worst cases in the resiliency evaluation, the interrupted consumers use all the devices they used in normal operation mode. Also, their energy consumption has not decreased. As a result, these two items help consumers achieve their desired level of comfort in this dire condition.

5. Conclusion

In this paper, a comprehensive program to optimize energy in normal operating conditions and emergency operating conditions is proposed. The energy optimization of household consumers is implemented through DRPHESs. The simulation results show that the RTP algorithm in the DRP improves the consumption pattern of household consumers

according to their convenience and preferences. As a result, the consumption pattern modification reduces the peak load, the total demand, and the consumer's payment and increases the load factor and the net surplus of consumers. Moreover, in emergency operation conditions, DRPHESs enable interrupted consumers to use all home appliances they used in normal operation conditions by the energy stored in their HESSs. The DN energy management is implemented using SHSRDE. The results show that the application of this program improves the voltage profile, reduces the lines' transmitted power and costs of the utility company, and increases social welfare and system security. In addition, in emergency operation conditions, SHSRDE significantly increases the ability of the DN to restore interrupted loads by converting the faulted part of the DN into several self-sufficient virtual microgrids. Consequently, the system's resiliency is considerably improved. However, the implementation of the proposed model of the article requires smart network infrastructure to manage and coordinate various distribution network components and smart home appliances. Furthermore, systems with high memory and processing power are needed to process and implement the proposed algorithms. The basic application of implementing the proposed model in future smart grids is to bring the interruption hours of electric power supply to consumers as close to zero as possible. To continue the work in the future, it is possible to examine and evaluate more precisely the behavior of consumers from the perspective of the economy of the power system. This would provide valuable information on how to increase the price elasticity of household consumers' demand. Furthermore, providing an algorithm for implementing the proposed framework through autonomous management of the smart grid during emergencies will greatly increase the speed of the load restoration process.

CRedit authorship contribution statement

Motahhar Tehrani Nowbandegani: Data curation, Investigation, Writing – original draft. **Mehrdad Setayesh Nazar:** Conceptualization, Methodology, Validation. **Mohammad Sadegh Javadi:** Formal analysis, Validation. **João P.S. Catalão:** Supervision, Writing – review & editing.

Declaration of competing interest

The authors declare that they have no known competing financial interests or personal relationships that could have appeared to influence the work reported in this paper.

Data availability

Data will be made available on request.

Acknowledgements

This work was partially supported by R&D Unit SYSTEC - Base (UIDB/00147/2020) and Programmatic (UIDB/00147/2020) funds - and Associate Laboratory ARISE - Advanced Production and Intelligent Systems (LA/P/0112/2020), funded by national funds through the FCT/MCTES (PIDDAC). Also, Mohammad Sadegh Javadi acknowledges FCT for his contract funding provided through 2021.01052.CEECIND.

References

- [1] Igder MA, Liang X. Service restoration using deep reinforcement learning and dynamic microgrid formation in distribution networks. *IEEE Trans Ind Appl* 2023 Jun 20. <https://ieeexplore.ieee.org/document/10158030>.
- [2] Wang C, Yan M, Pang K, Wen F, Teng F. Cyber-physical interdependent restoration scheduling for active distribution network via ad hoc wireless communication. *IEEE Trans Smart Grid* 2023 Feb 22. <https://ieeexplore.ieee.org/document/10050344>.

- [3] Mujjuni F, Betts TR, Blanchard RE. Evaluation of Power Systems Resilience to Extreme Weather Events: A Review of Methods and Assumptions. IEEE Access. 2023 Aug 14. <https://ieeexplore.ieee.org/document/10216278>.
- [4] Arefifar SA, Alam MS, Hamadi A. A Review on Self-Healing in Modern Power Distribution Systems. Journal of Modern Power Systems and Clean Energy. 2023 Jan 5. <https://ieeexplore.ieee.org/document/10007796>.
- [5] Liu F, Chen C, Lin C, Li G, Xie H, Bie Z. Utilizing aggregated distributed renewable energy sources with control coordination for resilient distribution system restoration. IEEE Trans Sustainable Energy 2023 Feb 6;14(2):1043–56. <https://ieeexplore.ieee.org/document/10038625>.
- [6] Menazzi M, Qin C, Srivastava AK. Enabling resiliency through outage management and data-driven real-time aggregated DERs. IEEE Trans Ind Appl 2023 Jun 14. <https://ieeexplore.ieee.org/document/9455050>.
- [7] Su J, Zhang H, Liu H, Yu L, Tan Z. Membership-function-based secondary frequency regulation for distributed energy resources in islanded microgrids with communication delay compensation. IEEE Trans Sustainable Energy 2023 Apr 11. <https://ieeexplore.ieee.org/document/10098785>.
- [8] Heidari-Akhijahani A, Butler-Purry KL. Phase Unbalance Impacts on Black-Start Service Restoration of Distribution Networks. In2023 IEEE Texas Power and Energy Conference (TPEC) 2023 Feb 13 (pp. 1-6). IEEE. <https://ieeexplore.ieee.org/document/10078630>.
- [9] Erenoglu AK, Sancar S, Terzi İS, Erdinç O, Shafie-Khah M, Catalão JP. Resiliency-driven multi-step critical load restoration strategy integrating on-call electric vehicle fleet management services. IEEE Trans Smart Grid 2022 Mar 1;13(4): 3118–32. <https://ieeexplore.ieee.org/document/9723455>.
- [10] Mohan GN, Bhende CN, Srivastava AK. Intelligent control of battery storage for resiliency enhancement of distribution system. IEEE Syst J 2021 Jun 15;16(2): 2229–39. <https://ieeexplore.ieee.org/document/9455050>.
- [11] Jia L, Pannala S, Kandaperumal G, Srivastava A. Coordinating energy resources in an islanded microgrid for economic and resilient operation. IEEE Trans Ind Appl 2022 Mar 1;58(3):3054–63. <https://ieeexplore.ieee.org/document/9723547>.
- [12] Gargari MZ, Hagh MT, Zadeh SG. Preventive scheduling of a multi-energy microgrid with mobile energy storage to enhance the resiliency of the system. Energy 2023 Jan;15(263):125597. <https://www.sciencedirect.com/science/article/abs/pii/S0360544222024835?via%3Dihub>.
- [13] Nowbandegani MT, Nazar MS, Shafie-khah M, Catalão JP. Demand response program integrated with electrical energy storage Systems for Residential Consumers. IEEE Syst J 2022 Feb 16;16(3):4313–24. <https://ieeexplore.ieee.org/document/9714457>.
- [14] Home-Ortiz JM, Melgar-Dominguez OD, Javadi MS, Mantovani JR, Catalão JP. Improvement of the distribution systems resilience via operational resources and demand response. IEEE Trans Ind Appl 2022 Jul 12;58(5):5966–76. <https://ieeexplore.ieee.org/document/9827489>.
- [15] Deng Y, Mu Y, Wang X, Jin S, He K, Jia H, et al. Two-stage residential community energy management utilizing EVs and household load flexibility under grid outage event. Energy Rep 2023 Mar;1(9):337–44. <https://www.sciencedirect.com/science/article/pii/S2352484722023496?via%3Dihub>.
- [16] Zeng Y, Han Y, Zhang D. A deep learning-based microgrid market modeling with planning assumptions. Comput Electr Eng 2022 May;110(10):107858. <https://www.sciencedirect.com/science/article/abs/pii/S0045790622001501?via%3Dihub>.
- [17] Wang K, Xue Y, Guo Q, Shahidehpour M, Zhou Q, Wang B, et al. A coordinated reconfiguration strategy for multi-stage resilience enhancement in integrated power distribution and heating networks. IEEE Trans Smart Grid 2022 Dec 30. <https://ieeexplore.ieee.org/document/10004513>.
- [18] Lee J, Razeghi G, Samuelsen S. Generic microgrid controller with self-healing capabilities. Appl Energy 2022 Feb;15(308):118301. <https://www.sciencedirect.com/science/article/abs/pii/S0360261921015609?via%3Dihub>.
- [19] Imteaj A, Akbari V, Amini MH. A novel scalable reconfiguration model for the postdisaster network connectivity of resilient power distribution systems. Jan 20; 23(3):1200 Sensors 2023. <https://www.mdpi.com/1424-8220/23/3/1200>.
- [20] Zhang L, Zhang B, Tang W, Lu Y, Zhao C, Zhang Q. A coordinated restoration method of hybrid AC–DC distribution network with electric buses considering transportation system influence. IEEE Trans Ind Inf 2022 Mar 22;18(11):8236–46. <https://ieeexplore.ieee.org/document/9739824>.
- [21] Gazijahani FS, Salehi J, Shafie-khah M. Benefiting from energy-hub flexibilities to reinforce distribution system resilience: a pre-and post-disaster management model. IEEE Syst J 2022 Feb 10;16(2):3381–90. <https://ieeexplore.ieee.org/document/9709361>.
- [22] Ding T, Wang Z, Qu M, Wang Z, Shahidehpour M. A sequential black-start restoration model for resilient active distribution networks. IEEE Trans Power Syst 2022 Apr 4;37(4):3133–6. <https://ieeexplore.ieee.org/document/9748971>.
- [23] Kirschen DS, Strbac G. Fundamentals of power system economics. John Wiley & Sons; 2018 Sep 24. [https://books.google.co.uk/books?hl=en&lr=&id=I9hhDwAAQBAJ&oi=fnd&pg=PR1&dq=23-%09Kirschen,+D.+S.,+%26+Strbac,+G.+\(2018\).+Fundamentals+of+power+system+economics.+John+Wiley+%26+Sons.&ots=fTsoW-1XM&sig=1s34Z7P5n2s-VZGdJCh2yvm1X_A&redir_esc=y#v=onepage&q&f=false](https://books.google.co.uk/books?hl=en&lr=&id=I9hhDwAAQBAJ&oi=fnd&pg=PR1&dq=23-%09Kirschen,+D.+S.,+%26+Strbac,+G.+(2018).+Fundamentals+of+power+system+economics.+John+Wiley+%26+Sons.&ots=fTsoW-1XM&sig=1s34Z7P5n2s-VZGdJCh2yvm1X_A&redir_esc=y#v=onepage&q&f=false).
- [24] Niknam T, Zare M, Aghaei J. Scenario-based multiobjective volt/var control in distribution networks including renewable energy sources. IEEE Trans Power Delivery 2012 Sep 19;27(4):2004–19. <https://ieeexplore.ieee.org/document/6301796>.
- [25] Hodge BM, Lew D, Milligan M. Short-term load forecast error distributions and implications for renewable integration studies. In2013 IEEE Green Technologies Conference (GreenTech) 2013 Apr 4 (pp. 435-442). IEEE. <https://ieeexplore.ieee.org/document/6520086>.
- [26] Razali NM, Hashim AH. Backward reduction application for minimizing wind power scenarios in stochastic programming. In2010 4th International Power Engineering and Optimization Conference (PEOCO) 2010 Jun 23 (pp. 430-434). IEEE. <https://ieeexplore.ieee.org/document/5559252>.
- [27] Allan RN. Reliability evaluation of power systems. Springer Science & Business Media; 2013 Nov 11. [https://books.google.co.uk/books?hl=en&lr=&id=4QryBwAAQBAJ&oi=fnd&pg=PA16&dq=27-%09Allan,+R.+N.+\(2013\).+Reliability+evaluation+of+power+systems.+Springer+Science+%26+Business+Media.&ots=HqW2-05dJg&sig=AnOCVbbz-zDr2KRGEkZrJsViyM4&redir_esc=y#v=onepage&q=27-%09Allan%2C%20R.%20N.%20\(2013\).%20Reliability%20evaluation%20of%20power%20systems.%20Springer%20Science%20%26%20Business%20Media.&f=false](https://books.google.co.uk/books?hl=en&lr=&id=4QryBwAAQBAJ&oi=fnd&pg=PA16&dq=27-%09Allan,+R.+N.+(2013).+Reliability+evaluation+of+power+systems.+Springer+Science+%26+Business+Media.&ots=HqW2-05dJg&sig=AnOCVbbz-zDr2KRGEkZrJsViyM4&redir_esc=y#v=onepage&q=27-%09Allan%2C%20R.%20N.%20(2013).%20Reliability%20evaluation%20of%20power%20systems.%20Springer%20Science%20%26%20Business%20Media.&f=false).
- [28] Kersting WH. Radial distribution test feeders. IEEE Trans Power Syst 1991 Aug;6(3):975–85. <https://ieeexplore.ieee.org/document/119237>.
- [29] Cedar Lake Ventures, Inc, Climate and Average Weather Year Round in South San Jose Hills, California, United States, Average Hourly Temperature in the Summer in South San Jose Hills. Accessed: Aug. 10, 2023. [Online]. Available: <https://weatherspark.com/y/1971/Average-Weather-in-South-San-Jose-Hills-California-United-States-Year-Round#Sections-Temperature>.
- [30] Cedar Lake Ventures, Inc, Summer 2023 Weather History in Los Angeles California, United States, Wind Speed in the Summer of 2023 in Los Angeles. Accessed: Aug. 10, 2023. [Online]. Available: <https://weatherspark.com/h/s/1705/2023/1/Historical-Weather-Summer-2023-in-Los-Angeles-California-United-States>.
- [31] Solar Energy Local, Solar Power in Los Angeles, CA, Solar Energy Data in Los Angeles, CA. Accessed: Aug. 10, 2023. [Online]. Available: <https://www.solarenergylocal.com/states/california/los-angeles/#ref>.
- [32] U.S. Energy Information Administration (EIA). (2022, March.). Electric Power Monthly with Data for January 2022. U.S. Department of Energy, Washington, DC 20585. [Online]. Available: <https://www.eia.gov/electricity/monthly/>.
- [33] U.S. Energy Information Administration (EIA). (2022.). ICE Wholesale Electricity Data. U.S. Department of Energy, Washington, DC & Intercontinental Exchange, Inc, U.S. [Online]. Available.
- [34] California ISO, Today's Outlook, Prices, California ISO Day-Ahead, Fifteen-Minute, and Real-Time Prices. Accessed: Aug. 10, 2023. [Online]. Available: <https://www.aiso.com/TodaysOutlook/Pages/prices.html>.
- [35] U.S. Energy Information Administration (EIA). (2022, March.). Levelized Costs of New Generation Resources in the Annual Energy Outlook 2022. U.S. Department of Energy, Washington, DC. [Online]. Available: https://www.eia.gov/outlooks/aeo/pdf/electricity_generation.pdf.
- [36] Federal Energy Regulatory Commission (FERC). (2005, Feb.). Principles for Efficient and Reliable Reactive Power Supply and Consumption. Federal Energy Regulatory Commission, Staff Report, Docket No. AD05-1-000, February 4, 2005, Washington, DC. [Online]. Available: https://hepg.hks.harvard.edu/sites/hwpi.harvard.edu/files/hepg/files/ferc_reactive_power_020405.pdf?m=1523368639.
- [37] Christopher Tufon, Alan G. Isemonger, Brendan Kirby, John Kueck, Fangxing (Fran) Li. (2008, June.). A Tariff for Reactive Power. OAK Ridge National Laboratory for the U.S. Department Of Energy (DOE) under contract DE-AC05_00OR22725, June 2008, Oak Ridge, Tennessee. [Online]. Available: <https://info.ornl.gov/sites/publications/files/Pub11472.pdf>.
- [38] U.S. Energy Information Administration (EIA). (2023.). Annual Electric Power Industry Report, Form EIA-861 detailed data files. U.S. Department of Energy, Washington, DC & Intercontinental Exchange, Inc, U.S. [Online]. Available: <https://www.eia.gov/electricity/data/eia861/>.